buffered saline and fixed for 10 min in 4% paraformaldehyde in phosphate-buffered saline. Cells were then permeabilized with 0.2% Triton X-100 in phosphate buffered saline for 10 min at room temperature. Samples were mounted onto coverslips with Pro-Long Gold Antifade reagent (Invitrogen) and were examined on a Zeiss LSM5 EXCITER confocal microscope. All images were acquired using an aplan-Apochrom at 63X with a 1.4-N.A. objective or at 100X with a 1.4-N.A. objective.

The Screening Method of Functional Residues of MyD88-TIR in IL-18 Signaling

HEK293T cells were transfected with pcDNA3.1+ control vector or pcDNA3.1+ myc-MyD88 TIR domain (wild-type or mutants), pcDNA3.1+ IL-18Rβ-AU1, NF-κB luciferase reporter vector, and Renilla luciferase reporter vector using Lipofectamine 2000 according to the manufacturer's instructions. These transfectants were stimulated with recombinant human IL-18 (100 ng/mL) for 6 hours. The luciferase reporter gene activities were also analyzed using a Dual-Luciferase Reporter Assay System (Promega). The statistical significance of the differences was determined using Dunnett's multiple comparison test. The statistical significance was assigned to be $P<0.05$.

Supporting Information

Figure S1 The surface electrostatic potential of the TIR domain structure models from the TIR domain containing adaptor proteins. These structure models were predicted from the template structure of the MyD88-TIR (PDB code: 2z5v) using Discovery Studio 2.6 software (Accelrys). TRAM and MAL have a largely acidic surface patch, while MyD88 has a largely basic surface patch.
(TIFF)

Figure S2 A schematic model of the two distinct regulation patterns in LPS induced TLR4 signaling and IL-18 signaling. MyD88 is efficiently delivered to receptor specific membrane regions by the membrane binding activities of the two associated molecules of Mal or TRAM so that it can form signal initiation complexes with activated TLR4 or IL-18 receptors. Upon stimulation, MyD88 starts to transmit signals through interactions with activated TLR4 or IL-18R, which triggers the phosphorylation cascade mediated by IRAKs and TRAF6.
(TIFF)

Acknowledgments

We thank Dr. T. Fukao, Dr. H. Kaneko, Dr. K Hirayama, and K. Kasahara for their advice and technical help. We thank Dr. S. Ki and Dr. T. Kokubo for their kind gift of vector samples.

Author Contributions

Conceived and designed the experiments: HO HT ZK MS N. Kondo. Performed the experiments: HO HT N. Kawamoto TK KK TY TF HN RW. Analyzed the data: HO HT RW MS. Wrote the paper: HO HT ZK RW MS.

References

1. Akira S, Uematsu S, Takeuchi O (2006) Pathogen recognition and innate immunity. Cell 124: 783–801.
2. Kawai T, Akira S (2007) Signaling to NF-kappaB by Toll-like receptors. Trends Mol Med 13: 460–469.
3. Bonnert TP, Garka KE, Parnet P, Sonoda G, Testa JR, et al. (1997) The cloning and characterization of human MyD88: a member of an IL-1 receptor related family. FEBS Lett 402: 81–84.
4. Lin SC, Lo YC, Wu H (2010) Helical assembly in the MyD88-IRAK4-IRAK2 complex in TLR/IL-1R signalling. Nature 465: 885–890.
5. Kagan JC, Medzhitov R (2006) Phosphoinositide-mediated adaptor recruitment controls Toll-like receptor signaling. Cell 125: 943–955.
6. Yamamoto M, Sato S, Hemmi H, Sanjo H, Uematsu S, et al. (2002) Essential role for TIRAP in activation of the signalling cascade shared by TLR2 and TLR4. Nature 420: 324–329.
7. Kenny EF, Talbot S, Gong M, Golenbock DT, Bryant CE, et al. (2009) MyD88 adaptor-like is not essential for TLR2 signaling and inhibits signaling by TLR3. J Immunol 183: 3642–3651.
8. Kagan JC, Su T, Horng T, Chow A, Akira S, et al. (2008) TRAM couples endocytosis of Toll-like receptor 4 to the induction of interferon-beta. Nat Immunol 9: 361–368.
9. Tanimura N, Saitoh S, Matsumoto F, Akashi-Takamura S, Miyake K (2008) Roles for LPS-dependent interaction and relocation of TLR4 and TRAM in TRIF-signaling. Biochem Biophys Res Commun 368: 94–99.
10. Rowe DC, McGettrick AF, Latz E, Monks BG, Gay NJ, et al. (2006) The myristoylation of TRIF-related adaptor molecule is essential for Toll-like receptor 4 signal transduction. Proc Natl Acad Sci U S A 103: 6299–6304.
11. Horng T, Barton GM, Flavell RA, Medzhitov R (2002) The adaptor molecule TIRAP provides signalling specificity for Toll-like receptors. Nature 420: 329–333.
12. Ohnishi H, Tochio H, Kato Z, Orii KE, Li A, et al. (2009) Structural basis for the multiple interactions of the MyD88 TIR domain in TLR4 signaling. Proc Natl Acad Sci U S A 106: 10260–10265.
13. O'Neill LA, Bowie AG (2007) The family of five: TIR-domain-containing adaptors in Toll-like receptor signalling. Nat Rev Immunol 7: 353–364.
14. Brown V, Brown RA, Ozinsky A, Hesselberth JR, Fields S (2006) Binding specificity of Toll-like receptor cytoplasmic domains. Eur J Immunol 36: 742–753.
15. Kato Z, Jee J, Shikano H, Mishima M, Ohki I, et al. (2003) The structure and binding mode of interleukin-18. Nat Struct Biol 10: 966–971.
16. Fitzgerald KA, Rowe DC, Barnes BJ, Caffrey DR, Visintin A, et al. (2003) LPS-TLR4 signaling to IRF-3/7 and NF-kappaB involves the toll adapters TRAM and TRIF. J Exp Med 198: 1043–1055.
17. Nishiya T, Kajita E, Horinouchi T, Nishimoto A, Miwa S (2007) Distinct roles of TIR and non-TIR regions in the subcellular localization and signaling properties of MyD88. FEBS Lett 581: 3223–3229.
18. Yamamoto M, Sato S, Hemmi H, Uematsu S, Hoshino K, et al. (2003) TRAM is specifically involved in the Toll-like receptor 4-mediated MyD88-independent signaling pathway. Nat Immunol 4: 1144–1150.
19. Bin LH, Xu LG, Shu HB (2003) TIRP, a novel Toll/interleukin-1 receptor (TIR) domain-containing adapter protein involved in TIR signaling. J Biol Chem 278: 24526–24532.
20. Oshiumi H, Sasai M, Shida K, Fujita T, Matsumoto M, et al. (2003) TIR-containing adapter molecule (TICAM)-2, a bridging adapter recruiting to toll-like receptor 4 TICAM-1 that induces interferon-beta. J Biol Chem 278: 49751–49762.
21. Dunne A, Ejdeback M, Ludidi PL, O'Neill LA, Gay NJ (2003) Structural complementarity of Toll/interleukin-1 receptor domains in Toll-like receptors and the adaptors Mal and MyD88. J Biol Chem 278: 41443–41451.
22. Sheedy FJ, O'Neill LA (2007) The Troll in Toll: Mal and Tram as bridges for TLR2 and TLR4 signaling. J Leukoc Biol 82: 196–203.
23. Sacre SM, Lundberg AM, Andreakos E, Taylor C, Feldmann M, et al. (2007) Selective use of TRAM in lipopolysaccharide (LPS) and lipoteichoic acid (LTA) induced NF-kappaB activation and cytokine production in primary human cells: TRAM is an adaptor for LPS and LTA signaling. J Immunol 178: 2148–2154.
24. Choi YJ, Im E, Chung HK, Pothoulakis C, Rhee SH (2010) TRIF mediates Toll-like receptor 5-induced signaling in intestinal epithelial cells. J Biol Chem 285: 37570–37578.
25. Medvedev AE, Piao W, Shoenfelt J, Rhee SH, Chen H, et al. (2007) Role of TLR4 tyrosine phosphorylation in signal transduction and endotoxin tolerance. J Biol Chem 282: 16042–16053.
26. Piao W, Song C, Chen H, Wahl LM, Fitzgerald KA, et al. (2008) Tyrosine Phosphorylation of MyD88 Adapter-like (Mal) Is Critical for Signal Transduction and Blocked in Endotoxin Tolerance. J Biol Chem 283: 3109–3119.
27. McGettrick AF, Brint EK, Palsson-McDermott EM, Rowe DC, Golenbock DT, et al. (2006) Trif-related adapter molecule is phosphorylated by PKC{epsilon} during Toll-like receptor 4 signaling. Proc Natl Acad Sci U S A 103: 9196–9201.
28. Seykora JT, Myat MM, Allen LA, Ravetch JV, Aderem A (1996) Molecular determinants of the myristoyl-electrostatic switch of MARCKS. J Biol Chem 271: 18797–18802.
29. Sancho-Shimizu V, Perez de Diego R, Lorenzo L, Halwani R, Alangari A, et al. (2011) Herpes simplex encephalitis in children with autosomal recessive and dominant TRIF deficiency. The Journal of clinical investigation 121: 4889–4902.
30. von Bernuth H, Picard C, Jin Z, Pankla R, Xiao H, et al. (2008) Pyogenic bacterial infections in humans with MyD88 deficiency. Science 321: 691–696.

JIMD Reports
DOI 10.1007/8904_2011_72

CASE REPORT

Three Japanese Patients with Beta-Ketothiolase Deficiency Who Share a Mutation, c.431A>C (H144P) in *ACAT1*: Subtle Abnormality in Urinary Organic Acid Analysis and Blood Acylcarnitine Analysis Using Tandem Mass Spectrometry

Toshiyuki Fukao • Shinsuke Maruyama • Toshihiro Ohura • Yuki Hasegawa • Mitsuo Toyoshima • Antti M. Haapalainen • Naomi Kuwada • Mari Imamura • Isao Yuasa • Rik K. Wierenga • Seiji Yamaguchi • Naomi Kondo

Received: 25 November 2010 / Revised: 10 June 2011 / Accepted: 20 June 2011 / Published online: 6 September 2011

Communicated by: K. Michael Gibson.

Competing interests: None declared.

T. Fukao (✉) · N. Kondo
Department of Pediatrics, Graduate School of Medicine, Gifu University, 1-1 Yanagido, Gifu 501-1194, Japan
e-mail: toshi-gif@umin.net

T. Fukao
Medical Information Sciences Division, United Graduate School of Drug Discovery and Medical Information Sciences, Gifu University, Gifu 501-1194, Japan

S. Maruyama · M. Toyoshima · N. Kuwada · M. Imamura
Department of Pediatrics, Graduate School of Medical and Dental Sciences, Kagoshima University, Kagoshima 890-8520, Japan

T. Ohura
Department of Pediatrics, Sendai City Hospital, Sendai, Miyagi 984-8501, Japan

Y. Hasegawa · S. Yamaguchi
Department of Pediatrics, Shimane University Faculty of Medicine, Izumo, Shimane 693-8501, Japan

A.M. Haapalainen · R.K. Wierenga
Department of Biochemistry and Biocenter Oulu, University of Oulu, Oulu 90014, Finland

M. Imamura
Kagoshima Prefectural Oshima Hospital, Naze, Kagoshima 894-0015, Japan

I. Yuasa
Division of Legal Medicine, Tottori University Faculty of Medicine, Yonago, Tottori 683-8503, Japan

Abstract Mitochondrial acetoacetyl-CoA thiolase (T2) deficiency affects both isoleucine catabolism and ketone body metabolism. The disorder is characterized by intermittent ketoacidotic episodes. We report three Japanese patients. One patient (GK69) experienced two ketoacidotic episodes at the age of 9 months and 3 years, and no further episodes until the age of 25 years. She had two uncomplicated pregnancies. GK69 was a compound heterozygote of the c.431A>C (H144P) and c.1168T>C (S390P) mutations in T2 (*ACAT1*) gene. She was not suspected of having T2 deficiency during her childhood, but she was diagnosed as T2 deficient at the age of 25 years by enzyme assay using fibroblasts. The other two patients were identical twin siblings who presented their first ketoacidotic crisis simultaneously at the age of 3 years 4 months. One of them (GK77b) died during the first crisis and the other (GK77) survived. Even during severe crises, C5-OH and C5:1 were within normal ranges in their blood acylcarnitine profiles and trace amounts of tiglylglycine and small amounts of 2-methyl-3-hydroxybutyrate were detected in their urinary organic acid profiles. They were H144P homozygotes. This H144P mutation has retained the highest residual T2 activity in the transient expression analysis of mutant cDNA thus far, while the S390P mutation did not retain any residual T2 activity. The "mild" H144P mutation may result in subtle profiles in blood acylcarnitine and urinary organic acid analyses. T2-deficient patients with "mild" mutations have severe ketoacidotic crises but their chemical phenotypes may be subtle even during acute crises.

Abbreviations

SCOT Succinyl-CoA:3-ketoacid CoA transferase
T2 Mitochondrial acetoacetyl-CoA thiolase

Introduction

Mitochondrial acetoacetyl-CoA thiolase (T2, gene symbol ACAT1) deficiency (OMIM 203750) is an autosomal recessive inborn error of metabolism that affects the catabolism of isoleucine and ketone bodies. This disorder, first described by Daum et al. (1971), is characterized by intermittent episodes of metabolic ketoacidosis associated with vomiting and unconsciousness often triggered by infections (Fukao et al. 2001). There are no clinical symptoms between episodes. Typical T2 deficiency is easily diagnosed by urinary organic acid analysis, characterized by massive excretion of tiglylglycine, 2-methyl-3-hydroxybutyrate and 2-methylacetoacetate both during ketoacidotic episodes and between episodes (Fukao et al. 2001, 2003). Diagnosis is confirmed by measurement of T2 activity on cultured skin fibroblasts (Robinson et al. 1979; Zhang et al. 2004). T2 deficiency is caused by mutations in the *ACAT1 (T2)* gene located on chromosome 11q22.3-q23.1 (Fukao et al. 1990; Kano et al. 1991). T2 deficiency is very heterogeneous at the genotype level, with at least 50 different mutations described (Fukao et al. 1995, 1997, 1998, 2001, 2002, 2003, 2007, 2008, 2010a, b; Wakazono et al. 1995; Nakamura et al. 2001; Zhang et al. 2004, 2006; Sakurai et al. 2007).

Some T2-deficient patients with mutations which retain some residual activity do not show typical urinary organic acid profiles (Fukao et al. 2001, 2003). We herein describe three Japanese patients with T2 deficiency whose H144P mutation retains significant residual activity. Their urinary organic acid and blood acylcarnitine profiles were atypical and subtle even during severe ketoacidotic crises.

Materials and Methods

Case Reports

GK69

This Japanese woman (GK69), born in 1984, developed severe metabolic acidosis at the age of 9 months. On admission to a third-level hospital, she was semicomatose, polypneic (48/min), and hypotonic. Laboratory values were: blood glucose 6.8 mmol/L, NH_3 92 μmol/L, blood pH 7.225, pCO_2 7.2 mmHg, bicarbonate 3 mmol/L, base excess −21.3, Na 153 mEq/L (normal range: 139–146), BUN 28.5 mg/dL (normal range: 10–18), and creatinine 1.1 mg/dL (normal range: 0.18–0.46). Metabolic acidosis was refractory to sodium bicarbonate therapy. Peritoneal dialysis was performed for 2 days. On the second hospital day, polypnea and unconsciousness disappeared and the blood gas data improved. Urinary organic acid analysis showed massive amounts of acetoacetate and 3-hydroxybutyrate with dicarboxylic aciduria. No increases in 2-methyl-3-hydroxybutyrate or tiglylglycine were noted, although this analysis was performed in an outside laboratory and no urine samples were available for reanalysis. At that time, T2 deficiency was excluded from differential diagnosis based on this organic acid data and the tentative diagnosis was succinyl-CoA:3-ketoacid CoA transferase (SCOT) deficiency. However, an enzyme assay for SCOT was not performed. At the age of 3 years, the patient had a similar but milder episode. Subsequently, she had no further ketoacidotic episodes. Growth and development were normal. She had two uncomplicated pregnancies.

Twin Siblings (GK77b and GK77)

GK77b is a twin Japanese boy. He was born at 36 weeks gestation weighing 2,400 g. His parents had no known consanguinity but both were from a small island in Amami islands in Japan. He experienced several febrile illnesses without ketoacidosis. However, at 3 years 4 months of age, after a 3-day history of fever, cough, and vomiting, he developed anorexia, lethargy, and polypnea. He was admitted to a local hospital. His blood glucose level was 2.3 mmol/L. Blood gas analysis was not performed. Hypoglycemia was corrected with intravenous glucose injection of 20 ml of 20% glucose solution followed by continuous infusion of a 2.6% glucose solution. About 30 h after admission, his condition worsened. Blood gas analysis revealed severe metabolic acidosis showed pH 6.88, pCO_2 6.1 mmHg, and bicarbonate 1.1 mmol/L. He was transferred to a regional hospital. On arrival at the hospital, he was unconscious with a heart rate of 168/min and respiratory rate of 39/min. Blood laboratory data were: WBC 19,050/μL, CRP 0.2 mg/dL (normal values: <0.15), BUN 36.2 mg/dL (normal range: 10–18) creatinine 0.5 mg/dL (normal range: 0.25–0.49), NH3 33.5 μmol/L, glucose 3.8 mmol/L, pH 7.17, pCO_2 20 mmHg, bicarbonate 6.3 mmol/L, base excess −22.4 mmol/L, and total ketone bodies 16.3 mmol/L. He received continuous infusion of 5% glucose solution at 3.4 mg/kg/min and sodium bicarbonate at 0.4–0.47 mEq/kg/h. However, unconsciousness and metabolic acidosis did not improve. On the fifth hospital day, he died before being transferred to a third-level hospital.

GK77 is the twin brother of GK77b. Pyloric stenosis was diagnosed at the age of 1 month and corrected surgically;

thereafter, he was well until 3 years 4 months of age. Two days after the onset of his twin brother, he developed frequent repeated vomiting after cough and nasal discharge. Therefore, he was admitted to the regional hospital at the same time as his twin. On admission, he was lethargic. Laboratory findings were: WBC 7,760/μL, CRP 0.5 mg/dL (normal values: <0.15), BUN 20.2 mg/dL (normal range: 10–18), creatinine 0.4 mg/dL (normal range: 0.25–0.49), glucose 3.7 mmol/L, NH3 25 μmol/L, blood pH 7.135, pCO_2 19.5 mmHg, bicarbonate 6.3 mmol/L, base excess −22.4 mmol/L, and total ketone bodies 10.1 mmol/L. He received a continuous infusion of 5% glucose solution at 3.4 mg/kg/min and sodium bicarbonate at 0.3 mEq/kg/h. On the third hospital day, his condition worsened and he was transferred to a third-level hospital. On admission, the blood gasses were pH 7.372, pCO_2 21.6 mmHg, bicarbonate 12.2 mmol/L, and base excess −11.2 mmol/L. A glucose infusion rate was further increased to 6.5 mg/kg/min with 10% glucose solution. Acidosis normalized with 9 h (pH 7.399, bicarbonate 21.7 mmol/L, base excess −2.6 mmol/L). Two days later, the urinary ketones became negative and he started eating.

GK77 is now 4 years 8 months and has experienced no further ketoacidotic episodes. The family has been advised to avoid fasting and to come to the local hospital if he has a high fever or appetite loss. His growth and development are within normal ranges.

Urinary Organic Acid Analysis and Acylcarnitine Analysis

Urine samples containing 0.2 mg of creatinine were used for our high risk screening of organic acids. As internal standards, 20 mg each of tropate (TA, C9), margarate (MGA, C17), and tetracosane (C24) were added to these samples. Trimethylsilylated samples were analyzed using capillary gas chromatography-mass spectrometry (QP 5050A, Shimadzu Co. Ltd., Kyoto, Japan), as described earlier (Kimura et al. 1999). The values of organic acids were expressed as the peak area (%) relative to IS-1 (margarate) on the mass chromatogram. Quantification of 2-methyl-3-hydroxybutyrate and tiglylglycine in urine samples from GK77b and GK77 was kindly done by Dr. Sass (Freiburg University) (Lehnert 1994). For comparison, quantification was also done in urine samples from T2-deficient patients whose urinary screening profiles had typical T2 deficient ones. We used urine sample in stable condition from GK01 who is a compound heterozygote of A333P and c.149delC (Fukao et al. 1998) and samples in acute and stable conditions from T2-deficient patients from India (GK(Ind)) in our high-risk screening. Blood spot and serum acylcarnitine analysis using tandem mass spectrometry was also done, as described (Kobayashi et al. 2007), and blood spot samples from GK75 and GK79, who are R208X homozygotes (Fukao et al. 2010b) were used as positive controls.

Enzyme Assay and Immunoblot Analysis Using Fibroblasts

Control and patients' fibroblasts were cultured in Eagle's minimum essential medium containing 10% fetal calf serum. Acetoacetyl-CoA thiolase activity was assayed, as described (Robinson et al. 1979; Zhang et al. 2004). We assayed acetoacetyl-CoA thiolase activity in the presence and absence of potassium-ion, since T2 is the only thiolase which is activated by the ion. Immunoblot analysis was done, as described (Fukao et al. 1997). In the cases of the controls, twofold serial dilution samples from 30 to 3.75 μg were electrophoresed together with samples (30 μg) of GK68 and GK77 to determine the amount of T2 protein in the patients' fibroblasts relative to that in the control fibroblasts.

Mutation Analysis

This study was approved by the Ethical Committee of the Graduate School of Medicine, Gifu University. Genomic DNA was extracted from fibroblasts using a SepaGene kit (Sanko Junyaku, Tokyo, Japan). Mutation screening was performed by PCR and direct sequencing of genomic fragments that included each exon and its surrounding intron sequences (Fukao et al. 1998). For GK77b and the parents, exon 5 was amplified from a dried blood spot 1.25 mm in diameter, which was used for tandem mass spectrometry, using Amplidirect Plus (Shimadzu Biotech, Tsukuba, Japan).

Restriction Enzyme Assay to Detect c.431A>C (H144P)

The c.431A>C (H144P) mutation creates a new BmgT120 I site (GGACC). DNAs from 110 Japanese controls were examined using a restriction enzyme assay, as follows.

A fragment (314 bp), including exon 5 and its surrounding introns, was amplified using the following primers:

In4 as (in intron, −69 to −48)5′-CATGCTCTATTAAG-TTCTGCAG-3′

In5 as (in intron, +137 to +119) 5′-ATCCAGACACTCT-TGAGCA-3′

An aliquot of the resulting amplicon was digested with BmgT120 I, then resolved on a 5% polyacrylamide gel. The c.431A fragment (wild-type) is 314-bp long and the c.421C fragment is cut into 162-bp and 152-bp fragments.

Transient Expression Analysis of Mutant cDNAs

Transient expression of T2 cDNAs was performed using a pCAGGS eukaryote expression vector (Niwa et al. 1991), as described (Sakurai et al. 2007). After transfection, cells were cultured at 37°C or 40°C for 48 h, then harvested and kept at −80°C until use. Cells were freeze-thawed and sonicated in 50 mM sodium phosphate (pH 8.0) and 0.1% Triton X-100. After centrifugation at 10,000 × g for 10 min, the supernatant was used in an enzyme assay for acetoacetyl-CoA thiolase activity and for immunoblot analysis.

Results and Discussion

Confirmation of the Diagnosis

GK69's fibroblasts were assayed for SCOT activity to confirm the diagnosis in 2008, when GK69 was 24 years old. As shown in Table 1, she was diagnosed as having T2 deficiency but not as having SCOT deficiency.

SCOT deficiency was first suspected in GK77 and GK77b, based on the following facts (1) Two of the four SCOT deficient Japanese families were from the Amami islands, the population of which is about 120,000. They were T435N homozygotes (Fukao et al. 2004). (2) The acylcarnitine profiles and urinary organic acid analysis during acute ketoacidotic crisis in both patients had no typical profile for T2 deficiency, as discussed below. As shown in Table 1, GK69's and GK77's fibroblasts had normal SCOT activity and a higher ratio (1.3) of acetoacetyl-CoA thiolase activity in the presence to the absence of potassium ions than typical T2-deficient fibroblasts (the ratio was around 1.0). Immunoblot analysis also showed a clearly detectable amount of T2 protein in GK77's fibroblasts, and a lower amount in GK69's fibroblasts. Densitometric analysis showed that the amounts of T2 protein in GK77 and GK69 were estimated to be 50% and 25% of control, respectively (Fig. 1).

Table 1 Acetoacetyl-CoA thiolase activities in the absence and presence of potassium ions

Fibroblasts	Acetoacetyl-CoA thiolase activity			SCOT activity
	$-K^+$	$+K^+$	$+K^+/-K^+$	
Controls ($n = 5$)	5.0 ± 0.7	10.8 ± 0.9	2.2 ± 0.3	6.7 ± 2.1
GK69	3.6 ± 0.5	4.1 ± 0.9	1.2 ± 0.1	4.7 ± 1.4
GK77	4.2 ± 0.3	5.8 ± 1.5	1.4 ± 0.3	3.9 ± 0.5
T2D	4.5 ± 1.4	4.7 ± 1.6	1.0 ± 0.1	5.6 ± 0.5

Enzyme activity is expressed as nmol/min/mg of protein. In cases of patients, enzyme assay was done three times and shows average ± SD. T2D, A disease control

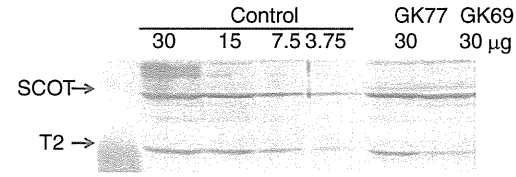

Fig. 1 Immunoblot analysis. In the cases of the controls, serial twofold dilutions from 30 to 3.75 μg were studied together with samples (30 μg) from GK68 and GK77. The first antibody was a mixture of an anti-T2 antibody and an anti-SCOT antibody. The positions of the bands for T2 and SCOT are indicated by *arrows*

Mutations and Their Effects on T2 Protein

Mutation screening revealed that GK69 was a compound heterozygote of c.431A>C (H144P) and c.1168T>C (S390P). Her mother had S390P heterozygously but did not have H144P. The father's DNA was not available for analysis. GK77 had an H144P mutation homozygously, shown by mutation screening at the genomic level. Their parents and GK77b were heterozygous carriers and a homozygote of H144P, respectively. The c.431A>C (H144P) mutation creates a BmgT120I site (GGACA to GGACC). We could not find c.431A>C (H144P) in the 110 Japanese controls using the restriction enzyme assay with BmgT120I.

We performed transient expression analysis of wild-type and mutant cDNAs in T2-deficient SV40-transformed fibroblasts. Following expression of T2 cDNAs for 48 h at 37°C, an enzyme assay and immunoblots were performed (Fig. 2a,b). The transfection of wild-type T2 cDNA produced high potassium ion-activated acetoacetyl-CoA thiolase activity (T2 activity), whereas that of mock cDNA produced no demonstrable enzyme activity at any temperature. The H144P mutant retained a residual T2 activity of ~25% of the wild-type value (Fig. 2a). The S390P mutant did not retain any residual T2 activity. In immunoblot analysis (Fig. 2b), the H144P mutant protein was detected, whereas no S390P protein was detected. The relative amount of the H144P mutant protein, as compared to the wild-type, was estimated to be 50%. Hence, the specific activity (unit/mg of T2 protein) of the H144P mutant protein was estimated to be about 50% of the wild type. Protein-folding and post-folding stability is predicted to vary with the incubation temperature. Hence, we also performed transient expression at 40°C for 48 h. The H144P mutant in expression at 40°C had a similar level of residual activity to that at 37°C.

We reported the tertiary structure of the human T2 tetramer (Haapalainen et al. 2007). Figure 3a shows the positions of the H144P and S390P mutations on the dimer.

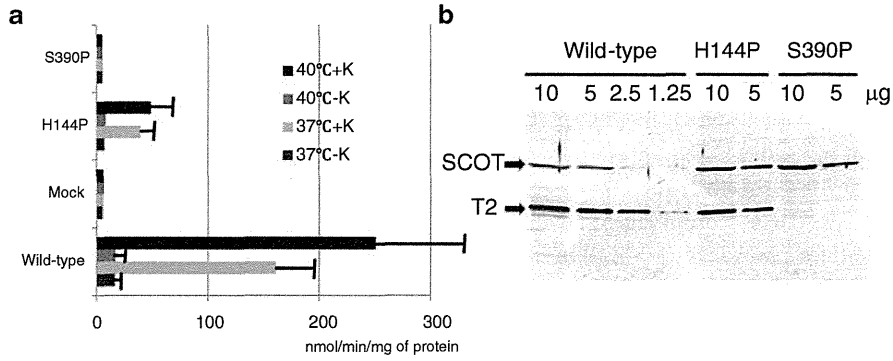

Fig. 2 Transient expression analysis of H144P and S390P mutant cDNAs. Transient expression analysis was performed at 40°C and 37°C. (**a**) Potassium ion-activated acetoacetyl-CoA thiolase assay. Acetoacetyl-CoA thiolase activity in the supernatant of the cell extract was measured. The mean values of acetoacetyl-CoA thiolase activity in the absence (−K) and presence (+K) of potassium ions are shown together with the SD of three independent experiments. (**b**) Immunoblot analysis. The protein amounts applied are indicated above the lanes. The first antibody was a mixture of an anti-T2 antibody and an anti-SCOT antibody. The positions of the bands for T2 and SCOT are indicated by *arrows*

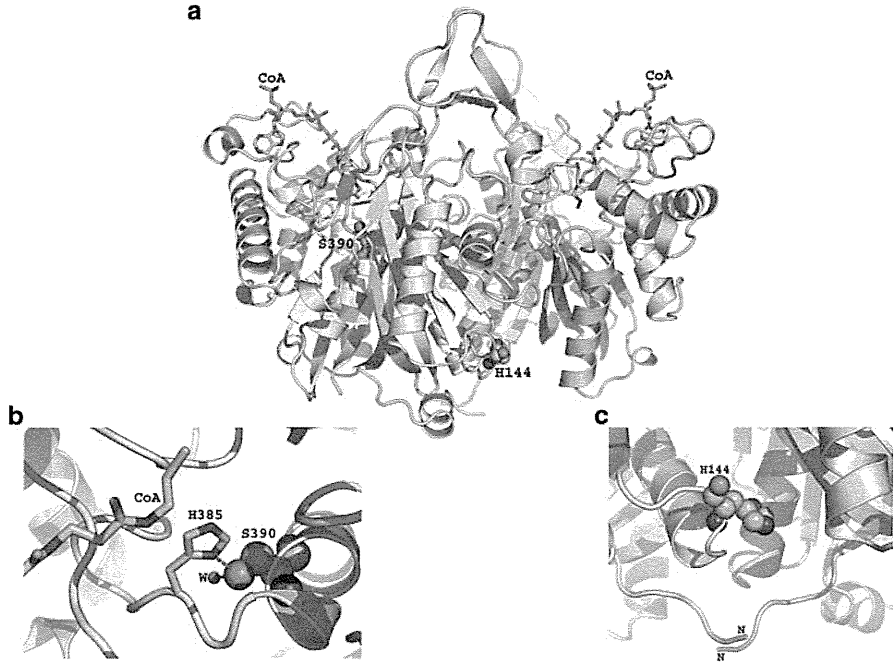

Fig. 3 The positions of H144P and S390P on the tertiary structure of human T2 dimers with substrates of coenzyme A

As seen in the figure, S390 is close to the active site and H144 is at the dimer interface close to the surface of the protein. Figure 3b shows a zoomed-in view around S390. This mutant is located at the active site. S390 is hydrogen-bonded to catalytic histidine, H385; it could be that this serine is needed to orient histidine in a way that the histidine can stabilize the transient negative charge of the substrate optimally. S390 is also hydrogen-bonded to a water molecule that is needed in stabilizing parts of the enzyme. So, if S390 is mutated into proline, these two hydrogen bonds do not exist. Hence, this S390P is expected to bring about a serious change in T2 catalytic cavity. In our expression analysis, this S390P was also too unstable to detect mutant protein. Figure 3c shows a zoomed-in view at the dimer interface. H144 is interacting with the residues of the neighboring subunit. If this residue is mutated into Pro, there is less dimeric interaction, which in turn might destabilize the overall structure. Since this residue is far from the active site and substrate binding site, it is difficult to explain why this H144P mutant had reduced specific activity in transient expression analysis from the viewpoint of structural analysis.

Urinary Organic Acid Analysis

GK69 was first suspected to having T2 deficiency as a probable diagnosis; however, urinary organic acid analysis at the first ketoacidotic crisis indicated no characteristic profile for T2 deficiency such as elevated 2-methyl-3-hydroxybutyrate and tiglylglycine in 1985 (no data was available). The results of the urinary organic acid analysis of our patients are shown in comparison with those of typical T2-deficient patients, GK01 and GK(Ind) (Table 2, Fig. 4). At the age of 24 years when her condition was stable, GK69's urinary organic acid analysis showed that there were only trace amounts of 2-methyl-3-hydroxybutyrate and tiglylglycine (Table 2). In our screening, this low level of tiglylglycine was difficult to detect. Urinary organic acid analysis during the acute crises of GK77 and GK77b showed huge amounts of 3-hydroxybutyrate and acetoacetate with elevated 2-methyl-3-hydroxybutyrate but only trace amounts of tiglylglycine. The levels of 2-methyl-3-hydroxybutyrate and tiglylglycine during a stable condition in GK77 are similar with those in GK69.

In cases of typical T2-deficient patients, it is easy to suspect T2 deficiency based on large amounts of 2-methyl-3-hydroxybutyrate and tiglylglycine as shown in Fig. 4. However, even in cases of trace amounts of tiglylglycine (possibly under the detection limit), T2 deficiency cannot be excluded. An H144P mutation, which retained high residual activity, may contribute to atypical profiles in the presented cases. These findings strengthen our previous observations that some T2-deficient patients with mutations, which retain some residual activity do not show typical urinary organic acid profiles (Fukao et al. 2001, 2003).

Table 2 Quantitative analysis of urinary organic acid analysis during acute crises and stable conditions

Patients	Acute crises		Stable conditions	
	2M3HB	Tiglylglycine	2M3HB	Tiglylglycine
GK69	NA	NA	14.0	13.3
GK77b	405.7	45.8	NA	NA
GK77	160.2	6.7	27.3	14.8
GK01	NA	NA	399.1	732.1
GK(Ind)	484.6	503.9	195.1	797.6
Controls ($n = 42$)			10.7 ± 7.6	24.6 ± 14.6

Values are expressed as mmol/mol creatinine

NA means that samples were not available for the analysis. GK01 is a compound heterozygote of c.149delC and A333P, which retained no residual activity (Fukao et al. 1998). GK(Ind) indicates a patient with typical T2-deficient profiles of urinary organic acids in our screening

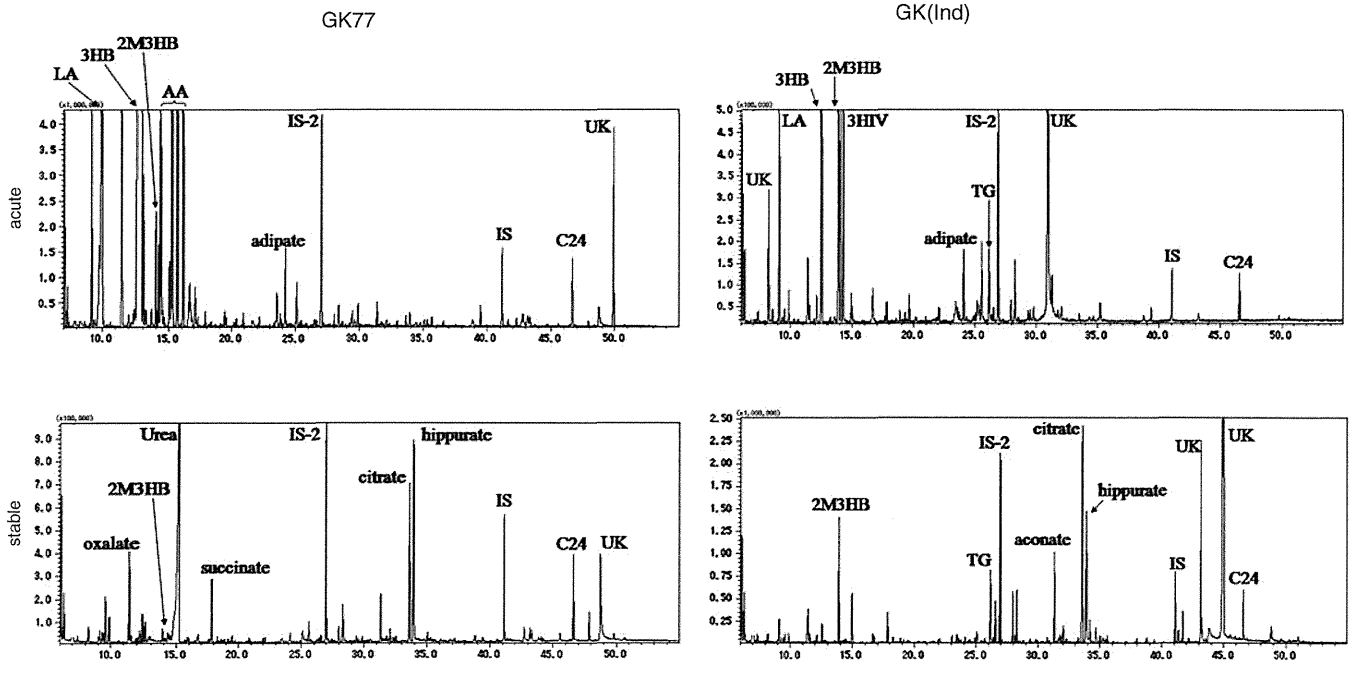

Fig. 4 Urinary organic acid profiles of GK77 during the acute episode and an asymptomatic period in comparison with those of a typical T2-deficient patient (GK(Ind)). *LA* Lactate, *3HB* 3-OH-butyrate, *3HIV* 3-OH-isovalerate, *AA* Acetoacetate, *2M3HB* 2-Methyl-3-OH-butyrate, *TG* Tiglylglycine, *IS-2* and *IS* Internal standards, *UK* Unknown. Since acetoacetate is unstable and samples from GK(Ind) were shipped on filter papers after thoroughly drying, the levels of acetoacetate are likely underestimated

Table 3 C5-OH and C5:1 carnitines in blood filters and serum samples from GK77 and GK77b during acute crises

Patients	Dried blood spots		Serum	
	C5:1	C5-OH	C5:1	C5-OH
GK77b	0.027	0.11	ND	0.12
GK77	0.012	0.11	0.044	0.10
R208X homozygotes				
GK75 (acute)	0.89	2.89	NA	NA
GK79 (stable)	1.20	2.35	NA	NA
Controls ($n = 30$)				
Average ± SD	0.015 ± 0.016	0.26 ± 0.15	0.015 ± 0.013	0.059 ± 0.024

ND not detected, *NA* not applicable

The values are expressed as μmol/L

GK75 and GK79 are positive controls for T2 deficient patients who are R208X homozygotes (Fukao et al. 2010b)

Blood and Serum Acylcarnitine Analyses

Acylcarnitine analysis was done using samples during the acute crises of GK77 and GK77b. Table 3 shows the results in comparison with those of typical T2-deficient patients (R208X homozygotes) (Fukao et al. 2010b). C5:1 and C5OH elevation in blood spots, characteristic for T2 deficiency, was clearly detected in the samples from the typical T2-deficient patients but was absent in samples from GK77 and GK77b. We previously reported that the abnormality of the acylcarnitine profiles in T2-deficient patients with mutations which retain some residual activity is subtle during nonepisodic conditions (Fukao et al. 2003), but the present study clearly showed that it could be also subtle even during severe ketoacidotic episodes. This means that acylcarnitine analysis using blood spots cannot detect some T2-deficient patients like GK77 and GK77b. Serum acylcarnitine analysis might detect elevation of these compounds to some extent, but we need to analyze more cases to clarify the usefulness of serum acylcarnitine analysis in such T2-deficient patients with mutations which retain some residual activity.

T2 deficiency cannot be excluded even if acylcarnitine profiles during acute episodes are within normal ranges. Careful evaluation of urinary organic acids, especially for the presence of 2-methyl-3-hydroxybutyrate, is necessary not to overlook T2 deficiency.

Clinical Issues

Since they were confirmed as identical twins by DNA analysis (data not shown), their genetic backgrounds were identical and most environmental factors were also very similar between them. One died during the ketoacidotic crisis and the other survived.

In Japan, intravenous infusion therapy for vomiting, appetite loss, and dehydration is commonly performed with commercially available initial infusion solution, such as Solita T1 (2.6% glucose) followed by maintenance solution, such as Solita T2 and T3 (4.3% glucose). These solutions are effective for physiological ketosis. However, in the case of T2 deficiency, a higher concentration of glucose may be necessary. Accordingly, we had the impression that GK77 became much better after the glucose concentration was changed from 5% to 10%. In the case of prolonged ketoacidosis, consideration should be given to increasing the infusion rate of glucose to ensure high normal blood glucose level to suppress ketone body synthesis and isoleucine catabolism via insulin secretion.

Acknowledgments We thank professor Jörn Oliver Sass (Freiburg Univ) for quantification of urinary 2-methyl-3-hydroxybutyrate and tiglylglycine, Drs Hironori Kobayashi and Yuichi Mushimoto (Shimane University) for urinary organic acid analysis and tandem mass analysis, Dr Tamayo Ishikawa (Kagoshima University) for patients' care, and Ms Keiko Murase and Ms Naomi Sakaguchi (Gifu University) for technical assistance. We also thank Paul Langman, PhD for his assistance with scientific English usage.

This study was in part supported by Health and Labor Science Research Grants for Research on Intractable Diseases and for Research on Children and Families from The Ministry of Health, Labor and Welfare of Japan and by a Grant-in-Aid for Scientific Research from the Ministry of Education, Science, Sports and Culture of Japan.

Concise One-Sentence Take-Home Message

Patients with beta-ketothiolase deficiency having a mutation which retains some residual activity showed subtle abnormality in urinary organic acid analysis and blood acylcarnitine analysis even during acute ketoacidotic episodes.

Details of the Contributions of Individual Authors

Toshiyuki Fukao and Naomi Kondo performed the enzyme assays, immunoblot/mutation analysis, and expression analysis of cDNAs. Toshiyuki Fukao mainly wrote this manuscript. Shinsuke Maruyama, Toshihiro Ohura, Mitsuo Toyoshima, Naomi Kuwada, and Mari Imamura are the physicians responsible for the patients. Yuki Hasegawa and Seiji Yamaguchi performed gas chromatography-mass spectrometry and tandem mass spectrometry analyses and first suspected the disorder. Isao Yuasa confirmed GK77 and 77b as identical twins by DNA analyses. Antti M Haapalainen and Rik K Wierenga analyzed the tertiary structural effects of the mutations.

References to Electronic Databases

Alpha-methylacetoacetic acidura, mitochondrial acetoacetyl-CoA thiolase deficiency (OMIM 203750, 607809)

Mitochondrial acetoacetyl-CoA thiolase, acetyl-CoA acetyltransferase 1 (EC 2.3.1.9)

ACAT1 gene (gene ID 38, NM_000019.3)

Details of Funding

This study was in part supported by Health and Labor Science Research Grants for Research on Intractable Diseases and Research on Children and Families from the Ministry of Health, Labor and Welfare of Japan and by a Grant-in-Aid for Scientific Research from the Ministry of Education, Science, Sports and Culture of Japan

Details of Ethics Approval

This study has been approved by the Ethical Committee of the Graduate School of Medicine, Gifu University.

References

Daum RS, Lamm PH, Mamer OA, Scriver CR (1971) A "new" disorder of isoleucine catabolism. Lancet 2:1289–1290

Fukao T, Yamaguchi S, Kano M et al (1990) Molecular cloning and sequence of the complementary DNA encoding human mitochondrial acetoacetyl-coenzyme A thiolase and study of the variant enzymes in cultured fibroblasts from patients with 3-ketothiolase deficiency. J Clin Invest 86:2086–2092

Fukao T, Yamaguchi S, Orii T, Hashimoto T (1995) Molecular basis of beta-ketothiolase deficiency: mutations and polymorphisms in the human mitochondrial acetoacetyl-coenzyme A thiolase gene. Hum Mutat 5:113–120

Fukao T, Song XQ, Mitchell GA et al (1997) Enzymes of ketone body utilization in human tissues: protein and messenger RNA levels of succinyl-coenzyme A (CoA):3-ketoacid CoA transferase and mitochondrial and cytosolic acetoacetyl-CoA thiolases. Pediatr Res 42:498–502

Fukao T, Nakamura H, Song XQ et al (1998) Characterization of N93S, I312T, and A333P missense mutations in two Japanese families with mitochondrial acetoacetyl-CoA thiolase deficiency. Hum Mutat 12:245–254

Fukao T, Scriver CR, Kondo N (2001) The clinical phenotype and outcome of mitochondrial acetoacetyl-CoA thiolase deficiency (beta-ketothiolase or T2 deficiency) in 26 enzymatically proved and mutation-defined patients. Mol Genet Metab 72:109–114

Fukao T, Nakamura H, Nakamura K et al (2002) Characterization of six mutations in five Spanish patients with mitochondrial acetoacetyl-CoA thiolase deficiency: effects of amino acid substitutions on tertiary structure. Mol Genet Metab 75: 235–243

Fukao T, Zhang GX, Sakura N et al (2003) The mitochondrial acetoacetyl-CoA thiolase (T2) deficiency in Japanese patients: urinary organic acid and blood acylcarnitine profiles under stable conditions have subtle abnormalities in T2-deficient patients with some residual T2 activity. J Inherit Metab Dis 26:423–431

Fukao T, Shintaku H, Kusubae R et al (2004) Patients homozygous for the T435N mutation of succinyl-CoA:3-ketoacid CoA Transferase (SCOT) do not show permanent ketosis. Pediatr Res 56:858–863

Fukao T, Zhang G, Rolland MO et al (2007) Identification of an Alu-mediated tandem duplication of exons 8 and 9 in a patient with mitochondrial acetoacetyl-CoA thiolase (T2) deficiency. Mol Genet Metab 92:375–378

Fukao T, Boneh A, Aoki Y, Kondo N (2008) A novel single-base substitution (c.1124A > G) that activates a 5-base upstream cryptic splice donor site within exon 11 in the human mitochondrial acetoacetyl-CoA thiolase gene. Mol Genet Metab 94:417–421

Fukao T, Horikawa R, Naiki Y et al (2010a) A novel mutation (c.951 C > T) in an exonic splicing enhancer results in exon 10 skipping in the human mitochondrial acetoacetyl-CoA thiolase gene. Mol Genet Metab 100:339–344

Fukao T, Nguyen HT, Nguyen NT et al (2010b) A common mutation, R208X, identified in Vietnamese patients with mitochondrial acetoacetyl-CoA thiolase (T2) deficiency. Mol Genet Metab 100:37–41

Haapalainen AM, Merilainen G, Pirila PL, Kondo N, Fukao T, Wierenga RK (2007) Crystallographic and kinetic studies of human mitochondrial acetoacetyl-CoA thiolase: the importance of potassium and chloride ions for its structure and function. Biochemistry 46:4305–4321

Kano M, Fukao T, Yamaguchi S, Orii T, Osumi T, Hashimoto T (1991) Structure and expression of the human mitochondrial acetoacetyl-CoA thiolase-encoding gene. Gene 109:285–290

Kimura M, Yamamoto T, Yamaguchi S (1999) Automated metabolic profiling and interpretation of GC/MS data for organic acidemia screening: a personal computer-based system. Tohoku J Exp Med 188:317–334

Kobayashi H, Hasegawa Y, Endo M, Purevsuren J, Yamaguchi S (2007) A retrospective ESI-MS/MS analysis of newborn blood spots from 18 symptomatic patients with organic acid and fatty acid oxidation disorders diagnosed either in infancy or in childhood. J Inherit Metab Dis 30:606

Lehnert W (1994) Long-term results of selective screening for inborn errors of metabolism. Eur J Pediatr 153:S9–S13

Nakamura K, Fukao T, Perez-Cerda C et al (2001) A novel single-base substitution (380 C > T) that activates a 5-base downstream cryptic splice-acceptor site within exon 5 in almost all transcripts in the human mitochondrial acetoacetyl-CoA thiolase gene. Mol Genet Metab 72:115–121

Niwa H, Yamamura K, Miyazaki J (1991) Efficient selection for high-expression transfectants with a novel eukaryotic vector. Gene 108:193–199

Robinson BH, Sherwood WG, Taylor J, Balfe JW, Mamer OA (1979) Acetoacetyl CoA thiolase deficiency: a cause of severe ketoacidosis in infancy simulating salicylism. J Pediatr 95:228–233

Sakurai S, Fukao T, Haapalainen AM et al (2007) Kinetic and expression analyses of seven novel mutations in mitochondrial acetoacetyl-CoA thiolase (T2): identification of a Km mutant and an analysis of the mutational sites in the structure. Mol Genet Metab 90:370–378

Wakazono A, Fukao T, Yamaguchi S et al (1995) Molecular, biochemical, and clinical characterization of mitochondrial acetoacetyl-coenzyme A thiolase deficiency in two further patients. Hum Mutat 5:34–42

Zhang GX, Fukao T, Rolland MO et al (2004) Mitochondrial acetoacetyl-CoA thiolase (T2) deficiency: T2-deficient patients with "mild" mutation(s) were previously misinterpreted as normal by the coupled assay with tiglyl-CoA. Pediatr Res 56:60–64

Zhang G, Fukao T, Sakurai S, Yamada K, Michael Gibson K, Kondo N (2006) Identification of Alu-mediated, large deletion-spanning exons 2–4 in a patient with mitochondrial acetoacetyl-CoA thiolase deficiency. Mol Genet Metab 89:222–226

Oncogene (2012) **31**, 4667–4676

www.nature.com/onc

ORIGINAL ARTICLE

Aberrant activation of ALK kinase by a novel truncated form ALK protein in neuroblastoma

J Okubo[1], J Takita[1,2], Y Chen[1], K Oki[1], R Nishimura[1], M Kato[1], M Sanada[3], M Hiwatari[1], Y Hayashi[4], T Igarashi[1] and S Ogawa[3]

Anaplastic lymphoma kinase (ALK) was originally identified from a rare subtype of non-Hodgkin's lymphomas carrying t(2;5)(p23;q35) translocation, where ALK was constitutively activated as a result of a fusion with nucleophosmin (NPM). Aberrant ALK fusion proteins were also generated in inflammatory fibrosarcoma and a subset of non-small-cell lung cancers, and these proteins are implicated in their pathogenesis. Recently, ALK has been demonstrated to be constitutively activated by gene mutations and/or amplifications in sporadic as well as familial cases of neuroblastoma. Here we describe another mechanism of aberrant ALK activation observed in a neuroblastoma-derived cell line (NB-1), in which a short-form ALK protein ($ALK^{del2\text{-}3}$) having a truncated extracellular domain is overexpressed because of amplification of an abnormal *ALK* gene that lacks exons 2 and 3. $ALK^{del2\text{-}3}$ was autophosphorylated in NB-1 cells as well as in $ALK^{del2\text{-}3}$-transduced cells and exhibited enhanced *in vitro* kinase activity compared with the wild-type kinase. $ALK^{del2\text{-}3}$-transduced NIH3T3 cells exhibited increased colony-forming capacity in soft agar and tumorigenicity in nude mice. RNAi-mediated ALK knockdown resulted in the growth suppression of $ALK^{del2\text{-}3}$-expressing cells, arguing for the oncogenic role of this mutant. Our findings provide a novel insight into the mechanism of deregulation of the ALK kinase and its roles in neuroblastoma pathogenesis.

Oncogene (2012) **31**, 4667–4676; doi:10.1038/onc.2011.616; published online 16 January 2012

Keywords: neuroblastoma; *ALK*; truncated form ALK; amplification

INTRODUCTION

Anaplastic lymphoma kinase (ALK) (OMIM: 105590) is an orphan receptor tyrosine kinase (RTK) that was initially characterized as a fusion partner of the nucleophosmin (NPM)-ALK chimeric protein associated with the t(2;5)(p23;q35) translocation in anaplastic large-cell lymphoma.[1,2] Subsequent studies have revealed that various ALK-containing fusion proteins with different fusion partners are generated in various solid tumors, such as inflammatory myofibroblastic tumors, non-small-cell lung cancer and squamous cell carcinoma of the esophagus.[3–6] Furthermore, recent genome-wide studies have revealed that *ALK* is activated by gene amplification and nucleotide mutations and is involved in the pathogenesis of both familial and sporadic neuroblastoma.[7–10]

Neuroblastoma is an intractable, solid tumor of childhood arising from the neural crest and can arise anywhere along the sympathetic nervous system.[11] The overall 5-year survival rate for neuroblastoma is ⩽40%, despite current intensive multimodality treatments.[12–14] Considering that *ALK* mutations preferentially involve advanced neuroblastoma with a poor outcome, the more relevant implication of these findings is that ALK inhibitors may improve the clinical outcome of children suffering from intractable neuroblastoma.

In this study, we demonstrated another mechanism of aberrant ALK activation in neuroblastoma, in which an abnormal *ALK* gene with a deletion of exons 2 and 3 was amplified in a neuroblastoma-derived cell line (NB-1), leading to high-level expression of an ALK protein variant with a truncated extracellular domain ($ALK^{del2\text{-}3}$). Furthermore, we demonstrated that $ALK^{del2\text{-}3}$ had constitutive kinase activity and showed a transforming capacity in NIH3T3 cells. Moreover, ALK inhibition experiments using small interfering RNA (siRNA)-mediated gene knockdown and the low-molecular-weight compound, TAE684, also supported the oncogenic role of $ALK^{del2\text{-}3}$. Our results will help elucidate the mechanism of aberrant activation of ALK kinase and the role of activated ALK in the pathogenesis of neuroblastoma.

RESULTS

Detection of a short-form ALK protein in NB-1 cells

To examine the status of ALK in neuroblastoma, western blotting analysis was performed with a panel of 24 neuroblastoma-derived cell lines (Table 1). Among the 24 samples examined, the NB-1 cell line showed high-level expression of an ALK protein having a low molecular weight of 208 kDa compared with the molecular weight of 220 kDa for the wild-type protein (Figure 1a). Subsequent sequencing and reverse transcription-polymerase chain reaction (RT-PCR) analysis of *ALK* messages from NB-1 cells revealed the presence of an aberrant *ALK* transcript with a 285-bp in-frame deletion in the 5′ region corresponding to exons 2 and 3 (Figures 1b and c), which should result in the production of an abnormal ALK protein with a truncated N-terminal extracellular domain. Using a primer set for exons 2 and 3, a 166-bp product was also detected in NB-1 cells, indicating the presence of the wild-type *ALK* allele in NB-1 cells (Figures 1b and c). The deletion spanned 224–318 amino acids (aa), including the N-terminal end of the first meprin A5 protein and receptor protein tyrosine phosphatase mu (MAM) domain (aa 264–427) (Figure 1d).[15,16] We analyzed full-length *ALK* cDNAs isolated from 71 primary neuroblastoma samples for possible nucleotide deletions using RT-PCR (Table 2), but no deletions were detected.

[1]Department of Pediatrics, Graduate School of Medicine, University of Tokyo, Tokyo, Japan; [2]Department of Cell Therapy and Transplantation Medicine, Graduate School of Medicine, University of Tokyo, Tokyo, Japan; [3]Cancer Genomics Project, Graduate School of Medicine, University of Tokyo, Tokyo, Japan and [4]Gunma Children's Medical Center, Maebashi, Japan. Correspondence: Dr J Takita, Cell Therapy and Transplantation Medicine, Graduate School of Medicine, University of Tokyo, 7-3-1, Hongo, Bunkyo-ku, Tokyo 113-8655, Japan. E-mail: jtakita-tky@umin.ac.jp
Received 22 May 2011; revised and accepted 29 November 2011; published online 16 January 2012

Table 1. Neuroblastoma cell lines used in this study

Cell line	*MYCN amplification*	*ALK status*
CHP-134	–	WT
GOTO	+	WT
LAN-1	+	F1174L
LAN-2	+	WT
LAN-5	+	R1275Q
NB-1	–	Amplification
NB-16	+	WT
NB-19	+	WT
NB-69	–	WT
NH-12	+	WT
SCMC-N2	+	F1174L
SCMC-N4	+	WT
SCMC-N5	+	K1062M
SJNB-1	–	WT
SJNB-2	+	R1275Q
SJNB-3	–	WT
SJNB-4	+	F1174L
SJNB-5	+	WT
SJNB-6	+	WT
SJNB-7	+	WT
SJNB-8	+	WT
SK-N-SH	–	F1174L
TGW	+	R1275Q
UTP-N-1	+	WT

Abbreviations: ALK, anaplastic lymphoma kinase; WT, wild type.

Structural abnormality of the *ALK* gene in NB-1 cells

As reported previously,[7] our single-nucleotide polymorphism array-based copy number analysis of NB-1 cells disclosed high-level gene amplification of the *ALK*-containing 2p24 segment. This should explain the high *ALK* expression observed in this cell line (Figures 1a and b). In particular, the genomic copy numbers within the 2p23 amplicon exhibited a transient decrease at three consecutive single-nucleotide polymorphisms (Chr2: 29 911 541–29 912 210), which corresponded to *ALK* intron 3, raising the possibility that a gene deletion involving exons 2 and 3 was responsible for the aberrant *ALK* transcript (Figure 2a). To confirm this, we performed Southern blot analysis of NB-1 genomic DNA using fragments exons 1–4 as probes (Figure 2b). As shown in Figures 2c–e, Southern blot analysis confirmed *ALK* gene amplification in NB-1 cells, as these blots showed high-intensity signals for each of the four *ALK*-specific probes in NB-1 cells compared with those in the controls. However, a significant difference was observed in the signal intensity between the fragments containing exons 1/4 and exons 2/3 in the NB-1 lanes, in which exons 1 and 4 showed 3.9- and 3.8-fold higher signals than exons 2 and 3, respectively. This result was confirmed by quantitative genomic PCR analysis using seven primer sets located within *ALK* exons 1–4 (Figure 2f). Taken together, these results indicate that the 2p23 amplicons were heterogeneous with regard to the species of *ALK* it contained, among which the predominant *ALK* allele had a deletion at exons 2 and 3, and these amplicons were responsible for the generation of $ALK^{del2\text{-}3}$.

Oncogenic potential of an aberrant short-form ALK protein

We next evaluated the oncogenic role of the truncated form of ALK found in NB-1 cells in terms of its kinase activity. As shown in Figure 3a, $ALK^{del2\text{-}3}$ was strongly phosphorylated in NB-1 cells, whereas the wild-type ALK expressed in NH-12 cells was unphosphorylated. Similar to the constitutive active F1174L ALK mutant when expressed in NIH3T3 cells, $ALK^{del2\text{-}3}$ had enhanced ALK phosphorylation compared with wild-type ALK (Figure 3b). Moreover, after anti-FLAG immunoprecipitation of FLAG-tagged ALK constructs, $ALK^{del2\text{-}3}$ and F1174L ALK mutants were strongly phosphorylated according to western blot analysis using a PY20 blot (Figure 3c). In addition, they exhibited enhanced kinase activity in an *in vitro* kinase assay using the YFF peptide as a substrate (Figure 3d). To confirm kinase activity of the $ALK^{del2\text{-}3}$ mutant, we further examined *in vitro* kinase activities of wild-type and mutant ALK-expressing NIH3T3 cells using a universal substrate. The immunoprecipitated FLAG-tagged $ALK^{del2\text{-}3}$ mutant showed significantly increased kinase activity (Supplementary Figure S1).

In an analysis of activated downstream signaling, significantly enhanced STAT3 phosphorylation was observed in $ALK^{del2\text{-}3}$ and F1174L mutants, whereas a significant increase in AKT phosphorylation was not detected in any samples (Figure 3e and Supplementary Figure S2). Extracellular regulated kinase (ERK) was probably phosphorylated in the F1174L mutant and wild-type ALK, but not in $ALK^{del2\text{-}3}$ (Figure 3e). The results of three independent experiments were quantified by densitometric scanning (Supplementary Figure S2).

We investigated the oncogenic potential of the $ALK^{del2\text{-}3}$ mutant in NIH3T3 cells, in terms of colony formation in soft agar and tumor generation in nude mice. As shown in Figures 4a and b, NIH3T3 cells that were stably transduced with $ALK^{del2\text{-}3}$ and ALK^{F1174L} produced a significantly higher numbers of colonies in soft agar than mock or wild-type *ALK*-transduced cells (Figures 4a and b). When inoculated into nude mice, the $ALK^{del2\text{-}3}$-transduced NIH3T3 cells invariably developed into subcutaneous tumors (5/5), whereas the mock and wild-type *ALK*-transfected cells did not develop into tumors (0/5) (Figure 4c).

$ALK^{del2\text{-}3}$ was retained in the endoplasmic reticulum

Among ALK signaling pathway molecules, STAT3 was only strongly phosphorylated by $ALK^{del2\text{-}3}$, suggesting that the $ALK^{del2\text{-}3}$ mutant was exclusively involved in the STAT3 pathway. It has been previously reported that intracellular fms-like tyrosine kinase-internal tandem duplication activation induces an aberrant downstream signaling outcome.[17] To determine whether $ALK^{del2\text{-}3}$ expresses at the cell surface and mediates signals from endoplasmic reticulum (ER), we analyzed localization and deglycosidation of $ALK^{del2\text{-}3}$ in NB-1 cells and wild-type ALK in NH-12 cells. Immunofluorescence staining revealed that ALK in NB-1 cells was almost colocalized with PDI, whereas ALK in NH-12 cells was largely located at the plasma membrane (Figure 5a). As shown in Supplementary Figure S4, colocalization of ALK and PDI was quantified using the Pearson's correlation coefficient. Moreover, to determine whether $ALK^{del2\text{-}3}$ was subjected to maturation of its oligosaccharides, we examined the endoglycosidase H sensitivity of ALK expressed in NB-1 and NH-12 cells. As shown in Figure 5b, $ALK^{del2\text{-}3}$ in NB-1 cells revealed the high sensitivity of endoglycosidase H compared with the wild-type ALK in NH-12 cells, suggesting that intercellular localization of $ALK^{del2\text{-}3}$ was associated with a defect in N-linked glycosylation.[18] These results indicate that $ALK^{del2\text{-}3}$ is mainly located at ER and aberrantly activates the STAT3 pathway from there.

Effect of ALK inhibition on cell growth in NB-1 cells

Finally, we examined the effect of ALK inhibition on NB-1 cell proliferation using the small-molecule ALK inhibitor TAE684 and siRNA-mediated ALK knockdown. NB-1 cell growth was effectively inhibited by TAE684 with a half maximal inhibitory concentration (IC_{50}) of 13 nM, which was similar to the IC_{50} for SK-N-SH (49 nM; an *ALK*-mutated TAE684-sensitive neuroblastoma cell line), but substantially lower than the IC_{50} for TGW cells with the ALK^{R1275Q} mutant (310 nM), the glioblastoma-derived cell line H4 with wild-type ALK (190 nM) and NIH3T3 cells with no ALK expression (380 nM) (Figure 6a). Similarly, siRNA-mediated knockdown of $ALK^{del2\text{-}3}$ in NB-1 cells resulted in significant suppression of cell proliferation compared with controls transfected with nonspecific

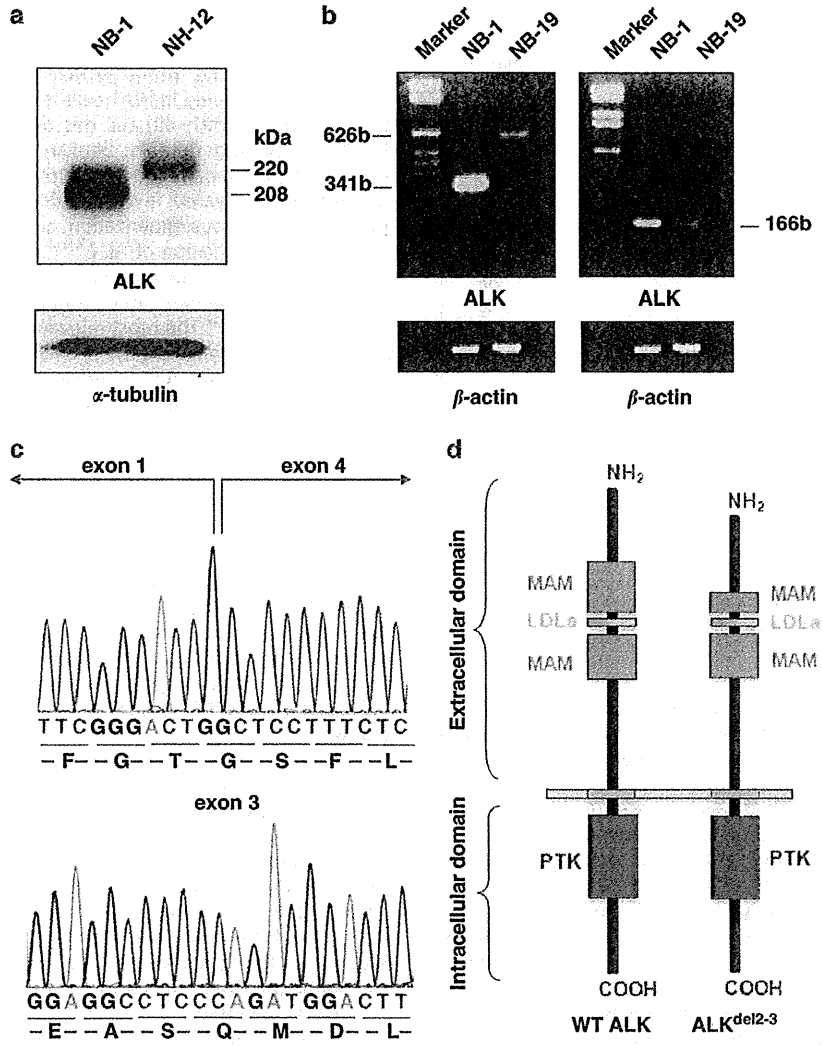

Figure 1. Detection of an aberrant truncated form of ALK in NB-1 cells. (**a**) Western blot analysis of ALK in neuroblastoma-derived cell lines. NB-1 cells strongly expressed the truncated form with a molecular mass of 208 kDa. In contrast, wild-type ALK-expressing neuroblastoma-derived cell lines (NH-12) revealed an ALK protein with a molecular mass of 220 kDa. α-Tubulin staining as loading control. (**b**) RT-PCR analysis of *ALK* exons 1–5 and exons 2 and 3 in the neuroblastoma cell lines. A short PCR product with 314 bp was detected in NB-1 cells, whereas much longer PCR products with 627 bp were detected in NB-19 cells with wild-type *ALK*. Wild-type *ALK* was detected in both NB-1 and NB-19 cells using *ALK* exon 2 and 3 primers. (**c**) Subsequent sequence analysis of *ALK* cDNA from NB-1. In-frame deletion in exons 2 and 3 was confirmed by direct sequencing. Sequencing of the PCR product detected by RT-PCR for *ALK* exons 2 and 3 confirmed the presence of wild-type *ALK* in NB-1 cells. Lower panel represents DNA sequencing for *ALK* exon 3 in NB-1 cells. (**d**) Schematic representation of the truncated form of aberrant ALK. The extracellular domain of ALK comprises two MAM domains (aa 264–427 and 480–626), one low-density lipoprotein class A (LDLa) motif (aa 453–471) and a glycine-rich region (aa 816–940) (Palmer *et al.*[30]). Because exons 2 and 3 of *ALK* implicate 224–318 aa, the in-frame deleted mutant led to a translational truncated form of the first MAM domain. PTK, protein tyrosine kinase.

siRNA, but the suppression apparently decreased in wild-type ALK-expressing NH-12 cells (Figures 6b and c). As shown in Supplementary Figure S3, significant inhibition was observed in NB-1 cells with ALK knockdown compared with that in the negative control ($P<0.05$, Mann-Whitney *U*-test).

DISCUSSION

Deregulated activation of ALK has been implicated in various human cancers through either generation of fusion proteins, overexpression or single amino-acid changes. In this study, we described a novel mechanism of oncogenic activation of *ALK* that operated in a neuroblastoma-derived cell line, NB-1. In NB-1 cells, an aberrant form of *ALK* that lacks exons 2 and 3 was amplified, leading to high-level expression of an N-terminal-truncated kinase, ALK^{del2-3}, and our functional studies confirmed the oncogenic role of ALK^{del2-3}. First, ALK^{del2-3} underwent autophosphorylation in NB-1 and NIH3T3 cells and demonstrated enhanced kinase activity, promoting downstream signaling pathways such as the STAT3 pathway. Second, ALK^{del2-3} promoted colony formation in soft agar and tumorigenicity when transduced into NIH3T3 cells in nude mice. Finally, inhibition of cell growth was observed when we treated NB-1 cells with TAE684, an ALK-specific kinase inhibitor, and siRNA-mediated gene knockdown. Unfortunately, screening of 71 primary neuroblastoma specimens and 23 neuroblastoma-derived cell lines did not identify a similar mechanism of ALK oncogenic activation in neuroblastoma; therefore, it is not a common mechanism for ALK activation in

Table 2. Neuroblastoma fresh tumor samples used in this study

Clinicopathological findings	*Samples*
Age (years)	
>1	41
<1	30
Stage	
1	16
2	11
3	12
4	29
4S	2
ND	1
MYCN status	
Amplification (+)	11
(−)	58
ND	2
ALK status	
Amplification	1
Mutation	6
Wild type	64
Total	71

Abbreviations: ALK, anaplastic lymphoma kinase; ND, not determined.

neuroblastoma. Nevertheless, the discovery of this unique ALK form will add to our knowledge with regard to the pathogenesis of neuroblastoma and will help to elucidate the mechanism of ALK activation.

Abnormal activation of RTK through a deletion in its extracellular domain has been documented in several cancers.[19–21] A common example of abnormal RTK activation is the epidermal growth factor receptor class III variant, which is present in a substantial proportion of malignant gliomas and other human cancers, but completely absent in normal tissues.[22,23] This variant results from a transcript having an 801-bp in-frame deletion of EGFR that corresponds to exons 2–7, which leads to the generation of a protein with a truncated extracellular domain.[21,24] Several molecular mechanisms have been implicated in the oncogenic pathway with epidermal growth factor receptor class III variant downstream signaling.[21,24] For example, in addition to ligand-independent self-dimerization, epidermal growth factor receptor class III variant has been shown to constitutively interact with adaptor proteins SHC and GRB2, which are involved in the recruitment of the RAS pathway.[25] The recepteur d'origine nantais (RON) RTK variant with a deletion in the first immunoglobulin-plexin transcription domain (RONΔ160) has also been considered as a constitutively activated kinase in several human cancers.[20,26] RON belongs to the MET proto-oncogene family, which plays a critical role in epithelial cell homeostasis and tumorigenic development.[27] RONΔ160 is derived from a *RON* mRNA transcript by alternative splicing that eliminates 109 aa residues from the extracellular domain of RON β-chain and is expressed in >50% of primary colon cancers and 90% of brain tumors, but not in any normal tissues.[26,28] The deleted 109 aa residues are encoded by exons 5/6, which constitute the first Immunoglobulin-plexin transcription domain in the RON β-chain.[26,28] The mechanism for the oncogenic activation of RONΔ160 is believed to be one in which the deletion in the extracellular domain causes conformational changes in the kinase and leads to spontaneous dimerization, which in turn causes constitutive receptor phosphorylation and increased intracellular signaling activation.[26,28,29]

The $ALK^{del2\text{-}3}$ variant consists of a 282-bp in-frame deletion of *ALK* that corresponds to 224–318 aa in the first MAM domain (Figure 1d). ALK is the sole RTK that contains MAM domains in its extracellular region.[30] Although MAM domains are thought to participate in cell–cell interactions, their significance in ALK function remains unclear.[15,16] Thus, the functional significance of MAM deletion in the truncated ALK is still elusive. As the deleted region of *ALK* detected in NB-1 cells is in close proximity to a ligand-binding domain (391–401 aa), this deletion may structurally alter the ligand-binding domain. Similar to epidermal growth factor receptor class III variant and RONΔ160, the $ALK^{del2\text{-}3}$ variant may be constitutively activated in a ligand-independent manner and/or through spontaneous dimerization, although the exact mechanism of constitutive activation of $ALK^{del2\text{-}3}$ is yet to be elucidated.

Oncogenic ALK transformation is mediated by interactions with downstream molecules that trigger a substantial intercellular signaling cascade.[31] The most relevant and best-characterized ALK downstream pathways are the RAS-ERK, JAK3-STAT3 and PI3K-AKT pathways.[31] Among ALK signaling molecules, STAT3 is only strongly phosphorylated by $ALK^{del2\text{-}3}$, suggesting that besides F1174L or K1062M ALK mutants,[7] $ALK^{del2\text{-}3}$ would be exclusively involved in the STAT3 pathway. Recently, it has been reported that the oncogenic mutant of fms-like tyrosine kinase-internal tandem duplication aberrantly activates STAT5 when localized at ER, but fails to activate MAPK and AKT signaling.[17] Thus, this raises the possibility that involvement of the STAT3 pathway in $ALK^{del2\text{-}3}$-expressing cells resembles the fms-like tyrosine kinase-internal tandem duplication mutant.[17] Immunofluorescence staining and the endoglycosidase H sensitivity assay revealed that $ALK^{del2\text{-}3}$ is mainly located at ER and aberrantly activates the STAT3 pathway from ER. Taken together, our results suggest that intracellular activation of $ALK^{del2\text{-}3}$ switches downstream signaling to the ALK pathway.[18]

Furthermore, ERK phosphorylation was similarly elevated in cells expressing wild-type or F1174L ALK. This may have been because of enhanced expression of exogenous wild-type *ALK* by retrovirus-mediated gene transfer. Schulte *et al.*[32] reported that the high level of wild-type ALK and mutant ALK expression has similar effects on the neuroblastoma biological phenotype, which may be related to tumor growth. Taken together, the results from our study and from the study by Schulte *et al.*[32] suggest that in addition to the ALK mutants, elevated wild-type ALK expression also mediates similar molecular functions that contribute to the malignant phenotype in neuroblastoma.

In summary, we found that an N-terminal-truncated ALK protein observed in a neuroblastoma-derived cell line (NB-1) is a novel oncogenic isoform of ALK. This study provides a better understanding of the molecular mechanism of pathogenesis of neuroblastoma as well as oncogenic roles of ALK pathway.

MATERIALS AND METHODS

Specimens

In all, 24 neuroblastoma cell lines were used in this study (Table 1). The SCMC-N series was established in our laboratory.[33] The SJNB series and UTP-N-1 cells were provided by Dr AT Look and Dr A Inoue, respectively. Other cell lines were obtained from the Japanese Cancer Resource Cell Bank (http://cellbank.nibio.go.jp/wwwjcrbj.htm). All cells were maintained in RPMI 1640 medium (Gibco, Grand Island, NY, USA) supplemented with 10% fetal bovine serum in a humidified atmosphere containing 5% CO_2 at 37 °C. Primary neuroblastoma specimens were obtained through surgery or biopsy from patients who were diagnosed with neuroblastoma and who were admitted to Tokyo University Hospital, Saitama Children's Medical Center or various other hospitals between November 1993 and October 2006. The patients were staged according to the International Neuroblastoma Staging System,[34] and the clinicopathological findings are listed in Table 2.

ALK expression analyses

Total cellular proteins were resolved on a 5–10% gradient sodium dodecyl sulfate-polyacrylamide gel and electrophoretically transferred onto

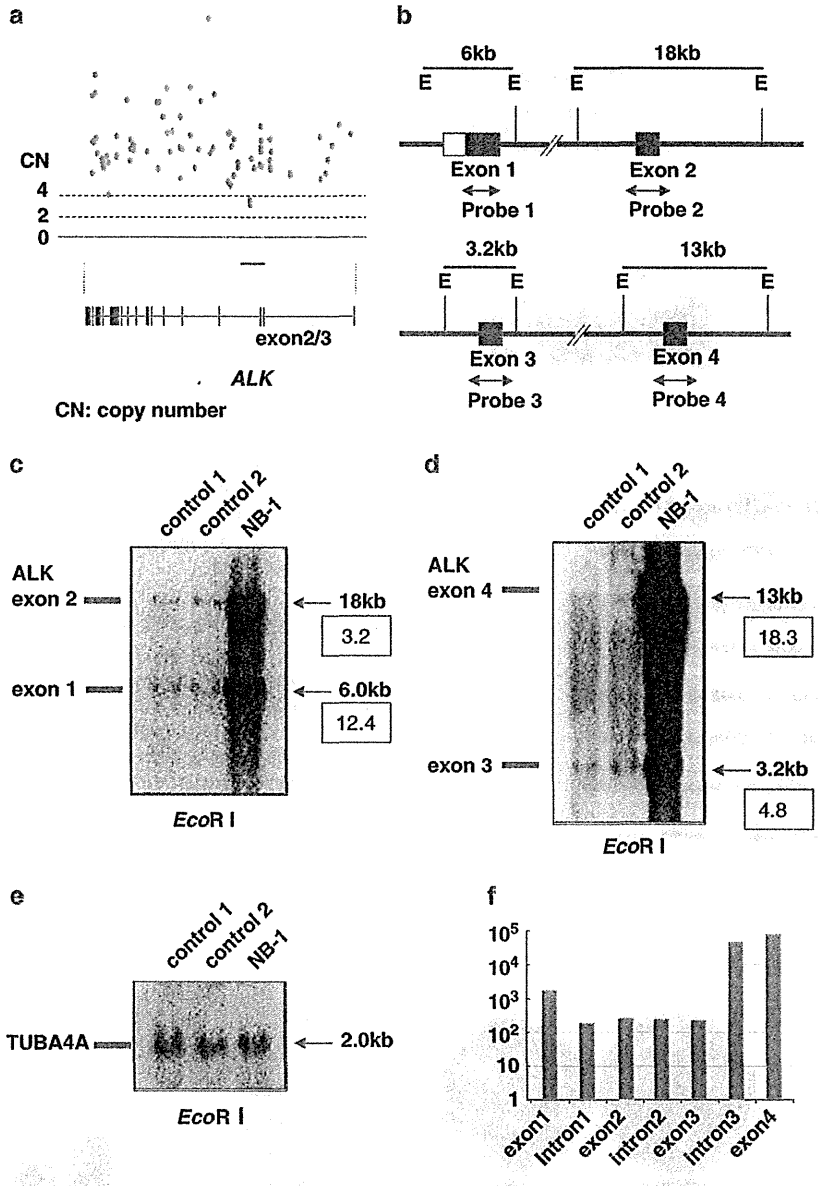

Figure 2. Genetic characteristics of the N-terminal-truncated form of ALK. (**a**) High-grade amplification of the *ALK* locus detected in NB-1 cells by single-nucleotide polymorphism array analysis (Affymetrix GeneChip 250k *Nspl*). Among the single-nucleotide polymorphism probes located within the *ALK* amplicon, three consecutive single-nucleotide polymorphism probes (Chr2: 29 911 541 and 29 912 210) located within *ALK* intron 3 showed relatively low signal intensities. The red line indicates the focal deletion within *ALK* intron 3. (**b**) Physical maps of *ALK* exons 1–4. The restriction sites and probe maps for *ALK* exons 1–4 are indicated. E: *EcoR*1. Arrows indicate probe positions. (**c**, **d**) Southern blot analysis using *ALK* exon 1–4 probes (**c**: exons 1 and 2; **d**: exons 3 and 4). Normal peripheral blood DNA was used as a germline control. Densitometric analysis was performed using the ImageQuant 400 and ImageQuant TL software version 7. (**e**) The TUBA4A probe was used as a loading control. (**f**) Quantitative genomic PCR analysis of *ALK* using seven primer sets located within *ALK* exons 1–4. The signal intensities of *ALK* introns 1 and 2 and exons 2 and 3 were lower compared with those of *ALK* exons 1 and 4 in NB-1 cells.

polyvinylidene difluoride membranes. After blocking with 5% milk in Tris-buffered saline containing 0.1% Tween (10 mM Tris-HCl (pH 7.4), 150 mM NaCl and 0.1% Tween-20), membranes were incubated for 1 h with primary antibody in TBS-T, washed and incubated for 12 h with primary antibody in 3% bovine serum albumin. The membranes were then washed again and incubated with anti-rabbit immunoglobulin G at room temperature for 1 h. Subsequently, they were extensively washed, and the proteins were visualized by enhanced chemiluminescence (Millipore, Bedford, MA, USA). Total RNA was extracted from the 24 cell lines and 71 frozen stocked tumors using Isogen reagent (Nippon Gene, Osaka, Japan) according to the manufacturer's instructions; the total RNA was analyzed by RT-PCR to synthesize cDNA using the SuperScript Preamplification System for first-strand cDNA synthesis (Life Technologies Inc., Rockville, MD, USA). RT-PCR analysis for *ALK* expression was performed as described previously,[7] using the primer sets listed in Table 3. cDNA concentration was equalized using *β-actin* expression as a control.

Southern blot analysis

High-molecular-weight DNA was prepared from cells according to standard procedures using the QIAamp DNA Mini kit (Qiagen, Valencia, CA, USA) and a modification of the protocol provided by the manufacturer.

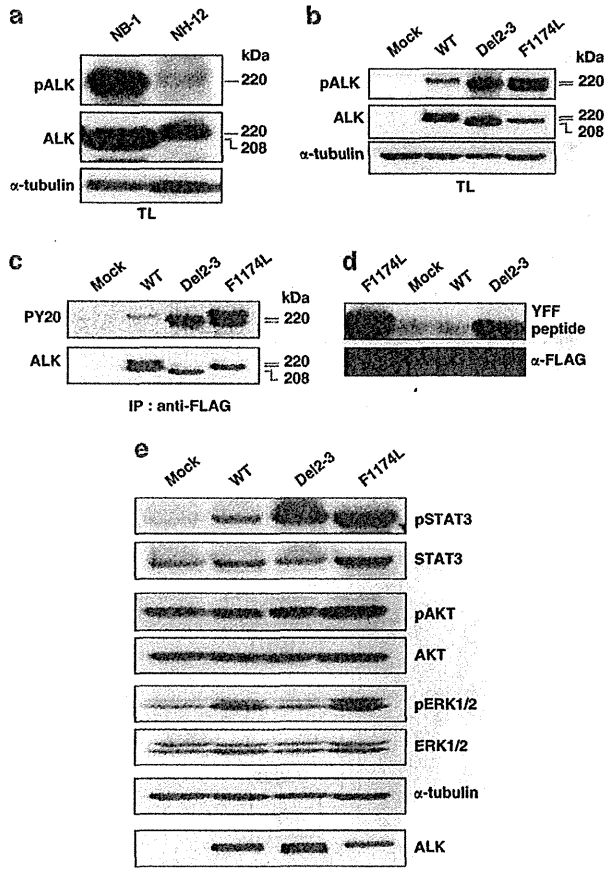

Figure 3. Kinase activities of ALK mutants and their downstream status. (**a**) Western blot analysis of ALK and phosphorylated ALK in NB-1 and NH-12 cells. NB-1 cells strongly expressed the truncated form of ALK and phosphorylated ALK compared with that in NH-12 cells. TL: Total cell lysates. (**b**) Western blot analysis of NIH3T3 cells stably expressing ALK mutants ($ALK^{del2\text{-}3}$ and ALK^{F1174L}) and wild-type ALK. (**c**) Stably expressed ALK mutants and wild-type ALK were immunoprecipitated with an anti-FLAG antibody and subjected to western blot analysis with anti-PY20. (**d**) *In vitro* kinase assay for wild-type ALK and its mutants using the synthetic YFF peptide as a substrate. (**e**) Western blot analysis of NIH3T3 cells stably expressing ALK mutants and wild-type ALK for their downstream effectors, STAT3 (pSTAT3), AKT (pAKT) and ERK (pERK). The total amount of each molecule is also shown together with an α-tubulin blot.

DNA was extracted from NB-1 cells and peripheral normal blood cells. For Southern blot analysis, 10 μg genomic DNA was restricted with *Eco*RI and loaded onto an agarose gel.[35] After electrophoresis, the DNA was transferred to polyvinylidene difluoride membranes and hybridized with radiolabeled probes for *ALK* exons 1–4 listed in Table 3. The signal intensity of each band was quantified and calculated using the ImageQuant 400 and ImageQuant TL software version 7 (GE Healthcare, Piscataway, NJ, USA).

Quantitative genomic PCR analysis

Quantitative genomic real-time PCR was performed using SYBR Green-based quantification (Bio-Rad Laboratories, Hercules, CA, USA). The standard curve method was used to calculate the target genome numbers in the NB-1 cell line. The relative target copy number was normalized to normal human genomic DNA as a calibrator. The primer sequences used for quantitative genomic PCR are shown in Table 3.

Transforming potential of ALK mutants

ALK^{WT}-FLAG and ALK^{F1174L}-FLAG were FLAG-tagged cDNAs for wild-type *ALK* and its F1174L mutant, respectively. FLAG-tagged cDNA for the

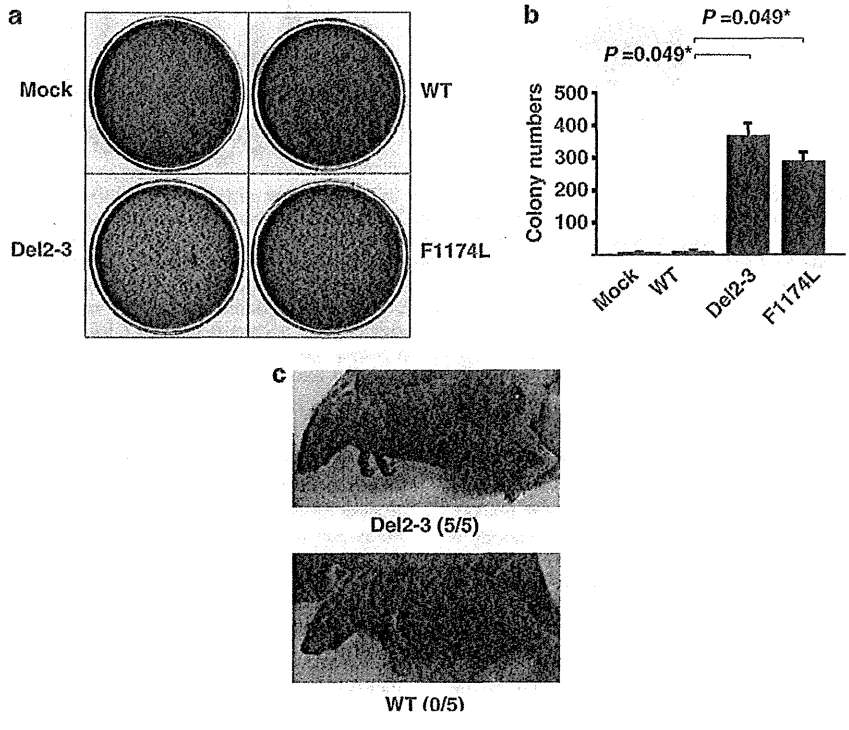

deletion mutant (*ALK*$^{del2\text{-}3}$-FLAG) was isolated from total RNA of NB-1 cells by high-fidelity PCR. After re-sequencing, each cDNA was constructed into the pcDNA3 expression plasmid and transfected into NIH3T3 cells using Effectene Transfection Reagents (Qiagen, Tokyo, Japan). Kinase assays were performed with stable clones in these constructs. For western blot analysis of mutant ALK and colony formation assays, NIH3T3 cells were stably transduced with wild-type and mutant ALK by retrovirus-mediated gene transfer. FLAG-tagged cDNA for wild-type and mutated ALK were then

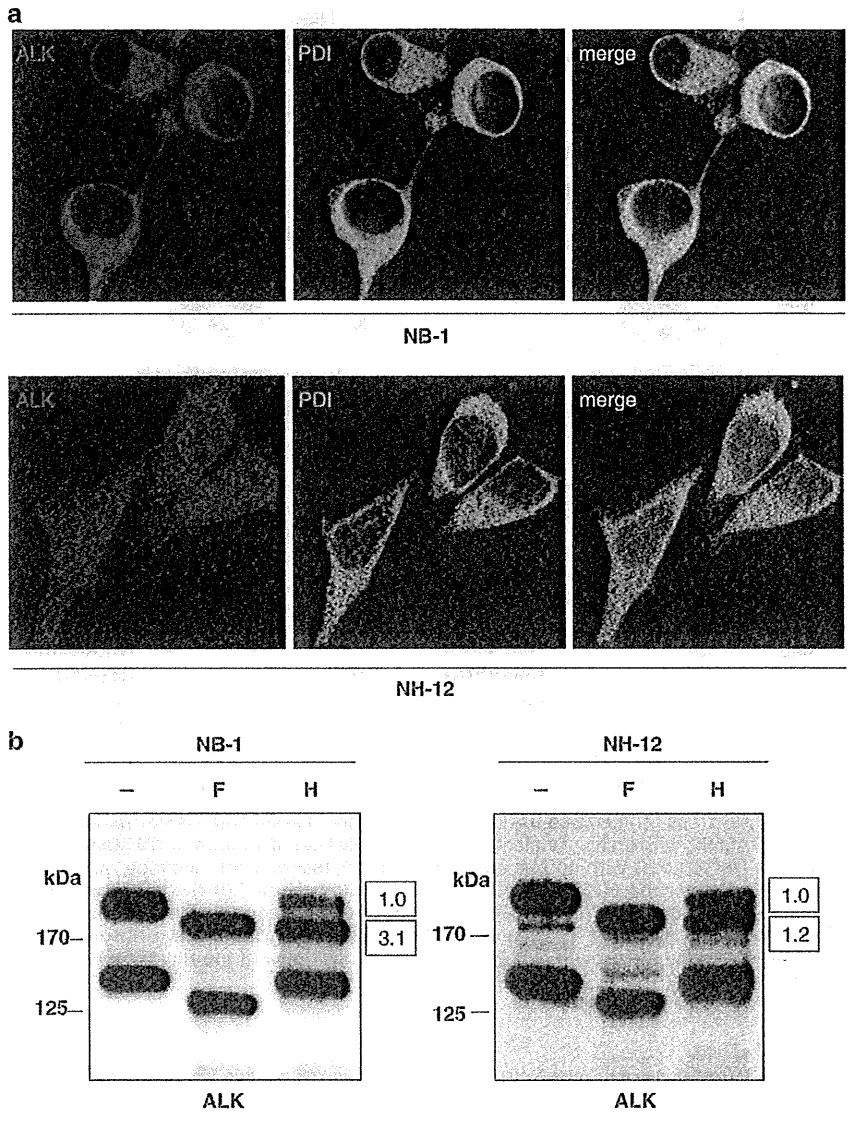

Figure 5. ER retention in the NB-1 neuroblastoma cell line and glycoprotein maturation. (**a**) Immunofluorescence confocal microscopy analysis of ALK ER localization in the neuroblastoma cell lines. The NB-1 and NH12 neuroblastoma cell lines were immunostained with the indicated antibodies and imaged using immunofluorescence microscopy to demonstrate ALK and PDI (ER-specific marker) colocalization. Cells were immunostained for ALK (red) and PDI (green), respectively. (**b**) The band of ALK$^{del2\text{-}3}$ protein of NB-1 cells is endoglycosidase H sensitive. Cell lysates from the NB-1 and NH12 neuroblastoma cell lines were incubated with N-glycosidase F (lane 2, F) and endoglycosidase H (lane 3, H). Deglycosidation profiles were compared with untreated cell lysates (lane 1). Digestion products were analyzed by western blot analysis using monoclonal anti-ALK. Signal intensities of bands in the lane endoglycosidase H were quantified by densitometric scanning using the ImageQuant 400 and ImageQuant TL software version 7. Signal intensity of approximate190 kDa band that revealed sensitivity to endoglycosidase H in NB-1 cells showed 3.1-fold higher than that of upper band.

Figure 4. Oncogenic role of the aberrant truncated form of ALK. (**a**) NIH3T3 cells stably expressing mutant kinases (ALK$^{del2\text{-}3}$ and ALK^{F1174L}) showed increased colony formation in soft agar compared with cells expressing wild-type kinase. (**b**) The average numbers of colonies in triplicate experiments are plotted. Standard deviation is indicated. Results showing significant differences compared with experiments using wild-type ALK are indicated by asterisks with *P*-values. (**c**) *In vivo* tumorigenicity assay in nude mice. Tumor formation assay in nude mice in which 1.0×10^7 NIH3T3 cells expressed wild-type ALK and the ALK$^{del2\text{-}3}$ mutant by the calcium phosphate method. Tumor formation was evaluated 21 days after inoculation.

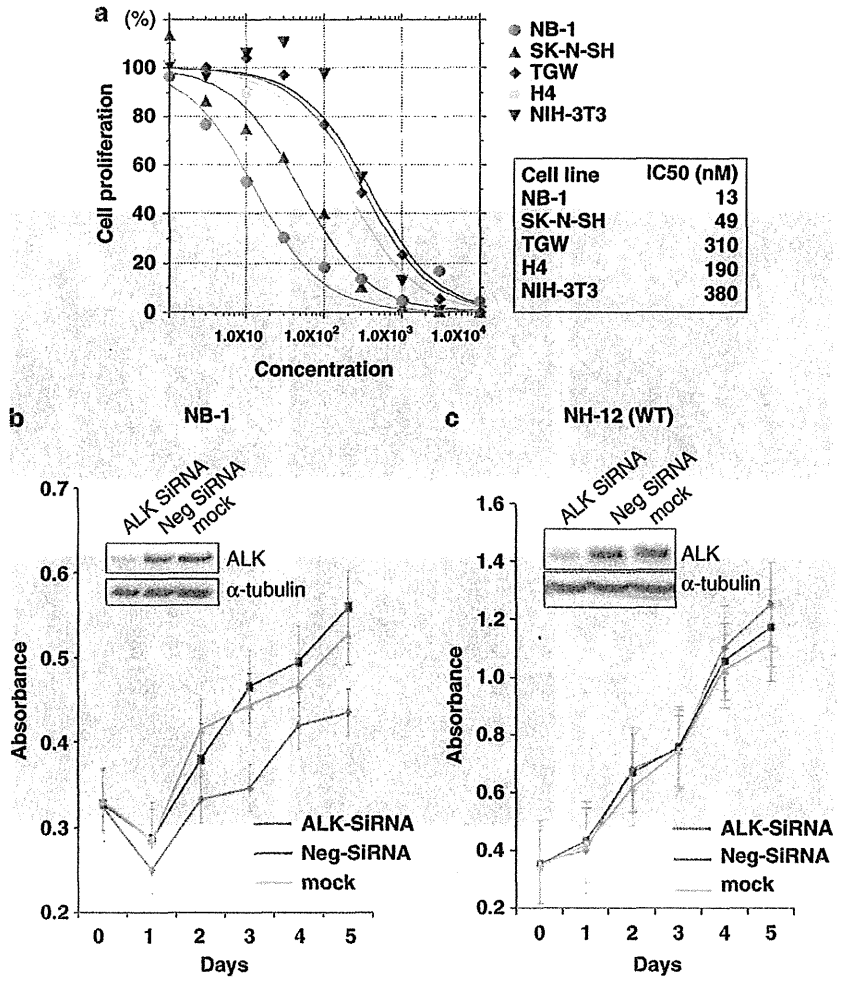

Figure 6. Effect of ALK inhibition on NB-1 cell proliferation using the ALK inhibitor TAE684 and siRNA-mediated ALK knockdown. (**a**) NB-1 cell growth was effectively inhibited by TAE684, with an IC_{50} similar to that for SK-N-SH (an *ALK*-mutated TAE684-sensitive neuroblastoma cell line), but substantially lower than that for NIH3T3 cells with no ALK expression. (**b**, **c**) Effect of RNAi-mediated ALK knockdown on cell proliferation in neuroblastoma cell lines expressing either the $ALK^{del2\text{-}3}$ mutant (NB-1) or wild-type ALK (NH-12). Cell growth was measured using the Cell Counting kit-8 after knockdown experiments using ALK-specific siRNAs, negative control siRNAs or mock experiments, in which absorbance was measured in triplicate and averaged for each assay. The mean ± s.d. of the average absorbance in three independent knockdown experiments was plotted to draw the growth curves. Successful knock down of the ALK protein was confirmed by anti-ALK blots using α-tubulin blots as controls.

constructed in the pGCDNsamIRESKO retrovirus vector. Vector plasmids were co-transfected with vesicular stomatitis virus-G cDNA into 293GP cells to obtain a retrovirus-containing supernatant, which was then transduced into 293GPG cells to stable cell lines capable of producing vesicular stomatitis virus-G-pseudotyped retroviral particles on induction.

Functional analyses of a short-form ALK

To evaluate the phosphorylation status of the ALK mutants, stable clone cell lysates were subjected to western blot analysis with anti-ALK and the antibody-specific pTyr1604 (Cell Signaling Technology, Danvers, MA, USA) of ALK. Immunoprecipitation with antibodies to FLAG (Sigma, St Louis, MO, USA) were subjected to western blot analysis with a generic antiphosphotyrosine antibody (PY20). Western blot analyses were also performed using anti-ERK1/2, anti-phospho-ERK1/2, anti-AKT, anti-phospho-AKT, anti-STAT3 and anti-phospho-STAT3 antibodies (Cell Signaling Technology). AKT and STAT3 phosphorylation signals were quantitated by densitometric scanning using the ImageQuant 400 and ImageQuant TL software version 7 (GE Healthcare). The *in vitro* kinase assay was performed with the synthetic YFF peptide (Operon Biotechnologies, Reutlingen, Germany), as described previously,[36] using stable clones in pcDNA vector constructs. We also used the *in vitro* kinase assay for wild-type and mutant *ALK* expression in NIH3T3 cells by retrovirus-mediated gene transfer using the poly-GluTyr peptide. Cell extracts were immunoprecipitated with anti-Flag antibody, and the expression was subjected to immunoblotting using anti-ALK antibody. ALK mutant kinase activity was measured using a non-radioactive isotope solid-phase enzyme-linked immunosorbent assay in the Universal Tyrosine Kinase Assay kit (Takara Bio, Osaka, Japan). Assays were performed in 40 mM Tris (pH 7.4), 20 mM $MgCl_2$, 2 mM dithiothreitol and 0.1 mg/ml bovine serum albumin buffer.

Transforming potential of short-form ALK

For colony assays, 1×10^3 stably transfected NIH3T3 cells were mixed in 0.4% agarose with 10% fetal bovine serum-Dulbecco's modified Eagle's medium and plated on 0.6% agarose-coated 35-mm dishes. After culturing for 14 days, colonies measuring 0.1 mm in diameter were counted. Colonies were quantified during triplicate experiments. Tumor formation

Table 3. Primer sets used in this study

	Primer sequence (5′→3′)		*Annealing temperature (°C)*
	Forward	*Reverse*	
RT-PCR analyses			
ALK exon 1/5	CTTCTCTTCCAGATCTTCGG	ATTCAGGGCAAAGAAGTCCAC	55
Exon 1/2	AAGCAGTTGGTGCTGGAGCT	TTTGACTTCCCCTGTGAGCT	55
Exon 2/4	CATAGCTCCTTGGAATCACC	ATGAGGAGCAGCAGTGAGCA	55
Exon 4/5-6	TTCTCAACACCTCAGCTGAC	ACTGCAGTGAAGGAACATCC	55
Exon 5/8-9	GAAACCGCAGCTTGTCTGCA	CGATCAAGAGCTCTCCATGT	55
Exon 8/12	AAGTGCTACAGTGACCAGTG	TAGCGGAGAGGACAAGATC	55
Exon 11/14	ATATCTCCATCAGCCTGGAC	AAGAACACCATGATGCGGTC	55
Exon 13/15-16	CCTGAAAGGCATCCAGATCT	AAGATGAAGGATGGAGTGCC	55
Exon 15/17	AATCCGTGTGAACAGAAGCG	TGGAGGAGGCGGAGGATATA	55
Exon 17/19-20	AAATCTTTGCAGGAGGGTGC	GCGTCTCCTGCATTGTGTCA	55
Exon 20/23	TTTCTCCGGCATCATGATTG	CTCATGGAAGCCCTGATCAT	55
Exon 23/26	TGCCTGAAGTGTGCTCTGAA	GATTGGAGACTTCGGGATGG	55
Exon 26/30	AGAAACTGCCTCTTGACCTG	GGACCCGGATGTAATCAACA	55
Exon 29/30	GGAGAGGATTGAATACTGCA	GTTGCACAAGGTCCACGGAT	55
Exon 30/30	TGCAGAGATCTCTGTTCGAG	GTTGCACAAGGTCCACGGAT	55
Exon 30/30	TAACGTTGCAACTGGGAGAC	GTTGCACAAGGTCCACGGAT	55
β-Actin	CTTCTACAATGAGCTGCGTG	TCATGAGGTAGTCAGTCAGC	55
Southern blot analyses			
ALK exon 1	AGAGTCTGGCAGTTGACTTC	TGCTCACAAACAGTCCCGAAG	60
Exon 2	TCAACTCAGTCTACTGGTGG	GGATATGGCAGACACAAAGC	60
Exon 3	AGCCCTGTGGTATTGACAAC	AGATGGGACTTGTCTTCCTC	60
Exon 4	AGAATGGAGGAAGAAGGCTG	GTAATTGCTCAACCTGGACC	60
TUBA4A	CTCTCACACTCTGGTATCTC	CTGACCATTAGCACAGTCTC	60
Quantitative genomic PCR analyses			
ALK exon 1	CTCAGCGAGCTGTTCAGTTG	CAGTCCCGAAGATCTGGAAG	55
Intron 1	CTGCTTGGTTCCTCACATCC	GTCTGAGTCATTGGCTAATCTCA	55
Exon 2	ACCCAAGCACATGGATCAG	GATGAGACAGGAAAGGGAAGG	55
Intron 2	GGTATACACGTGCCATGGTG	CCAAATACGGCATGTTCTCA	55
Exon 3	GGAGTGCAGCTTTGACTTCC	CTGGGCATCTCCTTAGAACG	55
Intron 3	TGGCATGATTGATTACCCAAG	CTGGAGATCACCCTTTGAGG	55
Exon 4	CAACACCTCAGCTGACTCCA	CTCTCTTGCAGCCTCGTTG	55

Abbreviations: ALK, anaplastic lymphoma kinase; RT-PCR, reverse transcription-polymerase chain reaction.

assay was performed in nude mice, in which 1.0×10^7 NIH3T3 cells expressing wild-type *ALK* and *ALK*$^{del2\text{-}3}$ mutant were injected by the calcium phosphate method. Tumor formation was evaluated 21 days after inoculation as described previously.[6]

Immunofluorescence

Cells were fixed for 10 min with 4% paraformaldehyde and washed three times with phosphate-buffered saline. After 1 h of blocking in phosphate-buffered saline containing 4% donkey serum and 0.1% Triton X-100/phosphate-buffered saline, the cells were incubated for 2 h in the same buffer with polyclonal anti-ALK (Santa Cruz Biotechnology, Santa Cruz, CA, USA) and monoclonal anti-PDI (Abcam, Cambridge, MA, USA), respectively. The cells were then washed three times with phosphate-buffered saline before and after incubation with anti-mouse IgG Alexa Fluor 488 and anti-rabbit IgG Alexa Fluor 594-conjugated secondary antibodies, respectively, (Invitrogen, Carlsbad, CA, USA). The cells were then mounted in Prolong Gold (Invitrogen). Confocal laser microscopy was performed using a Fluoview 10 000 confocal microscope (Olympus, Tokyo, Japan). Colocalization of ALK and PDI was quantified using the Pearson's correlation coefficient and determined through correlation analysis with a Fluoview 1000 software.[37]

Deglycosylation of ALK with N-glycosidase F, N-glycosidase H and O-glycosidase

Proteins from cell lysates obtained from neuroblastoma cell lines NB-1 and NH-12 were incubated with N-glycosidase F and endoglycosidase H for deglycosylation (New England Biolabs, Ipswich, MA, USA), following the manufacturer's instructions.[18] The samples were then used for immunoblotting with anti-ALK antibody. Signal intensities of bands in the lane endoglycosidase H were quantified by densitometric scanning using the ImageQuant 400 and ImageQuant TL software version 7.

ALK inhibition by an ALK inhibitor and siRNA-mediated knockdown in neuroblastoma cells

A partial *ALK*-deleted neuroblastoma-derived cell line (NB-1), *ALK*-mutated neuroblastoma-derived cell lines (SK-N-SH and TGW) and a glioblastoma-derived cell line (H4) were cultured with varying concentrations of the ALK inhibitor TAE684,[8] and cell growth was measured using the CellTiter-Glo Luminescent Cell Viability Assay (Promega, Tokyo, Japan). NIH3T3 cells were used as a control. The IC_{50} value of TAE684 against NB-1 cells was calculated by nonlinear regression (variable slope) using the GraphPad Prism 5 software (GraphPad, La Jolla, CA, USA). NB-1 and NH-12 cells with wild-type ALK were transfected with either an *ALK*-specific siRNA or a nonspecific siRNA, as described previously.[7] To assess the effect of ALK knockdown on cell growth, cells were seeded in 96-well plates at a concentration of 1.0×10^4 cells per well 24 h before transfection and assayed using the Cell Counting kit-8 (Dojindo, Kumamoto, Japan). We also performed an siRNA-mediated ALK knockdown cell proliferation assay using a cell counter and 6-well plates. These cells were seeded in 6-well plates at a concentration of 2.0×10^5 cells per well 24 h before transfection. The number of cells was counted after 72 h using cytorecon (ECI, Tokyo, Japan).

Statistical analyses

The Mann-Whitney *U*-test was used to compare the differences in colony formation as well as the effects of ALK knockdown on cell growth between wild-type and ALK mutants. Phosphorylation signals of downstream molecules were evaluated by Student's *t*-test.

CONFLICT OF INTEREST

The authors declare no conflict of interest.

ACKNOWLEDGEMENTS

We thank Mrs Matsumura, Mrs Hoshino, Mrs Yin, Miss Ogino and Mrs Saito for their excellent technical assistance. We would also thank Dr Tanaka, Dr Saito, Mr Shiosaka and Mrs Mori for useful advice concerning biological analysis; Dr AT Look, Harvard Medical University, and Dr A Inoue, St Jude Children's Research Hospital, for their generous gifts of neuroblastoma cell lines. This work was supported by Research on Measures for Intractable Diseases, Health and Labor Sciences Research Grants, Ministry of Health, Labor and Welfare, Research on Health Sciences focusing on Drug Innovation, the Japan Health Sciences Foundation and Core Research for Evolutional Science and Technology, Japan Science and Technology Agency.

REFERENCES

1 Morris SW, Kirstein MN, Valentine MB, Dittmer K, Shapiro DN, Look AT *et al.* Fusion of a kinase gene, ALK, to a nucleolar protein gene, NPM, in non-Hodgkins-lymphoma (Vol 263, PG 1281, 1994). *Science* 1995; **267**: 316-317.
2 Shiota M, Nakamura S, Ichinohasama R, Abe M, Akagi T, Takeshita M *et al.* Anaplastic large-cell lymphomas expressing the novel chimeric protein P80(NPM/ALK)-a distinct clinicopathological entity. *Blood* 1995; **86**: 1954-1960.
3 Griffin CA, Hawkins AL, Dvorak C, Henkle C, Ellingham T, Perlman EJ. Recurrent involvement of 2p23 in inflammatory myofibroblastic tumors. *Cancer Res* 1999; **59**: 2776-2780.
4 Jazii FR, Najafi Z, Malekzadeh R, Conrads TP, Ziaee AA, Abnet C *et al.* Identification of squamous cell carcinoma associated proteins by proteomics and loss of beta tropomyosin expression in esophageal cancer. *World J Gastroenterol* 2006; **12**: 7104-7112.
5 Rikova K, Guo A, Zeng Q, Possemato A, Yu J, Haack H *et al.* Global survey of phosphotyrosine signaling identifies oncogenic kinases in lung cancer. *Cell* 2007; **131**: 1190-1203.
6 Soda M, Choi YL, Enomoto M, Takada S, Yamashita Y, Ishikawa S *et al.* Identification of the transforming EML4-ALK fusion gene in non-small-cell lung cancer. *Nature* 2007; **448**: 561-5U3.
7 Chen YY, Takita J, Choi YL, Kato M, Ohira M, Sanada M *et al.* Oncogenic mutations of ALK kinase in neuroblastoma. *Nature* 2008; **455**: 971-U56.
8 George RE, Sanda T, Hanna M, Frohling S, Luther W, Zhang JM *et al.* Activating mutations in ALK provide a therapeutic target in neuroblastoma. *Nature* 2008; **455**: 975-978.
9 Janoueix-Lerosey I, Lequin D, Brugieres L, Ribeiro A, de Pontual L, Combaret V *et al.* Somatic and germline activating mutations of the ALK kinase receptor in neuroblastoma. *Nature* 2008; **455**: 967-U51.
10 Mosse YP, Laudenslager M, Longo L, Cole KA, Wood A, Attiyeh EF *et al.* Identification of ALK as a major familial neuroblastoma predisposition gene. *Nature* 2008; **455**: 930-U22.
11 Maris JM, Hogarty MD, Bagatell R, Cohn SL. Neuroblastoma. *Lancet* 2007; **369**: 2106-2120.
12 De Bernardi B, Nicolas B, Boni L, Indolfi P, Carli M, di Montezemolo LC *et al.* Disseminated neuroblastoma in children older than one year at diagnosis: comparable results with three consecutive high-dose protocols adopted by the Italian Co-Operative Group for Neuroblastoma. *J Clin Oncol* 2003; **21**: 1592-1601.
13 Matthay KK, Villablanca JG, Seeger RC, Stram DO, Harris RE, Ramsay NK *et al.* Treatment of high-risk neuroblastoma with intensive chemotherapy, radiotherapy, autologous bone marrow transplantation, and 13-*cis*-retinoic acid. *N Engl J Med* 1999; **341**: 1165-1173.
14 Pearson ADJ, Pinkerton CR, Lewis IJ, Imeson J, Ellershaw C, Machin D *et al.* High-dose rapid and standard induction chemotherapy for patients aged over 1 year with stage 4 neuroblastoma: a randomised trial. *Lancet Oncol* 2008; **9**: 247-256.
15 Beckmann G, Bork P. An adhesive domain detected in functionally diverse receptors. *Trends Biochem Sci* 1993; **18**: 40-41.
16 Loren CE, Englund C, Grabbe C, Hallberg B, Hunter T, Palmer RH. A crucial role for the anaplastic lymphoma kinase receptor tyrosine kinase in gut development in *Drosophila melanogaster*. *EMBO Rep* 2003; **4**: 781-786.
17 Choudhary C, Olsen JV, Brandts C, Cox J, Reddy PNG, Boehmer FD *et al.* Mislocalized activation of oncogenic RTKs switches downstream signaling outcomes. *Mol Cell* 2009; **36**: 326-339.
18 Mazot P, Cazes A, Boutterin MC, Figueiredo A, Raynal V, Combaret V *et al.* The constitutive activity of the ALK mutated at positions F1174 or R1275 impairs receptor trafficking. *Oncogene* 2011; **30**: 2017-2025.
19 Lemmon MA, Schlessinger J. Cell signaling by receptor tyrosine kinases. *Cell* 2010; **141**: 1117-1134.
20 Lu Y, Yao HP, Wang MH. Multiple variants of the RON receptor tyrosine kinase: biochemical properties, tumorigenic activities, and potential drug targets. *Cancer Lett* 2007; **257**: 157-164.
21 Pedersen MW, Meltorn M, Damstrup L, Poulsen HS. The type III epidermal growth factor receptor mutation-biological significance and potential target for anti-cancer therapy. *Ann Oncol* 2001; **12**: 745-760.
22 Ekstrand AJ, James CD, Cavenee WK, Seliger B, Pettersson RF, Collins VP. Genes for epidermal growth-factor receptor, transforming growth factor-alpha, and epidermal growth-factor and their expression in human gliomas *in vivo*. *Cancer Res* 1991; **51**: 2164-2172.
23 Wong AJ, Ruppert JM, Bigner SH, Grzeschik CH, Humphrey PA, Bigner DS *et al.* Structural alterations of the epidermal growth-factor receptor gene in human gliomas. *Proc Natl Acad Sci USA* 1992; **89**: 2965-2969.
24 Gan HK, Kaye AH, Luwor RB. The EGFRvIII variant in glioblastoma multiforme. *J Clin Neurosci* 2009; **16**: 748-754.
25 Prigent SA, Nagane M, Lin H, Huvar I, Boss GR, Feramisco JR *et al.* Enhanced tumorigenic behavior of glioblastoma cells expressing a truncated epidermal growth factor receptor is mediated through the Ras-Shc-Grb2 pathway. *J Biol Chem* 1996; **271**: 25639-25645.
26 Zhou YQ, He C, Chen YQ, Wang D, Wang MH. Altered expression of the RON receptor tyrosine kinase in primary human colorectal adenocarcinomas: generation of different splicing RON variants and their oncogenic potential. *Oncogene* 2003; **22**: 186-197.
27 Ronsin C, Muscatelli F, Mattei MG, Breathnach R. A novel putative receptor protein tyrosine kinase of the met family. *Oncogene* 1993; **8**: 1195-1202.
28 Wang MH, Kurtz AL, Chen YQ. Identification of a novel splicing product of the RON receptor tyrosine kinase in human colorectal carcinoma cells. *Carcinogenesis* 2000; **21**: 1507-1512.
29 Chen YQ, Zhou YQ, Angeloni D, Kurtz AL, Qiang XZ, Wang MH. Overexpression and activation of the RON receptor tyrosine kinase in a panel of human colorectal carcinoma cell lines. *Exp Cell Res* 2000; **261**: 229-238.
30 Palmer RH, Vernersson E, Grabbe C, Hallberg B. Anaplastic lymphoma kinase: signalling in development and disease. *Biochem J* 2009; **420**: 345-361.
31 Chiarle R, Voena C, Ambrogio C, Piva R, Inghirami G. The anaplastic lymphoma kinase in the pathogenesis of cancer. *Nat Rev Cancer* 2008; **8**: 11-23.
32 Schulte JH, Bachmann HS, Brockmeyer B, DePreter K, Oberthur A, Ackermann S *et al.* High ALK receptor tyrosine kinase expression supersedes ALK mutation as a determining factor of an unfavorable phenotype in primary neuroblastoma. *Clin Cancer Res* 2011; **17**: 5082-5092.
33 Takita J, Yang HW, Chen YY, Hanada R, Yamamoto K, Teitz T *et al.* Allelic imbalance on chromosome 2q and alterations of the caspase 8 gene in neuroblastoma. *Oncogene* 2001; **20**: 4424-4432.
34 Brodeur GM, Pritchard J, Berthold F, Carlsen NLT, Castel V, Castleberry RP *et al.* Revisions of the international criteria for neuroblastoma diagnosis, staging, and response to treatment. *J Clin Oncol* 1993; **11**: 1466-1477.
35 Takita J, Hayashi Y, Nakajima T, Adachi J, Tanaka T, Yamaguchi N *et al.* The p16 (CDKN2A) gene is involved in the growth of neuroblastoma cells and its expression is associated with prognosis of neuroblastoma patients. *Oncogene* 1998; **17**: 3137-3143.
36 Donella-Deana A, Marin O, Cesaro L, Gunby RH, Ferrarese A, Coluccia AML *et al.* Unique substrate specificity of anaplastic lymphoma kinase (ALK): development of phosphoacceptor peptides for the assay of ALK activity. *Biochemistry* 2005; **44**: 8533-8542.
37 Smith JL, McBride CM, Nataraj PS, Bartos DC, January CT, Delisle BP. Trafficking-deficient hERG K(+) channels linked to long QT syndrome are regulated by a microtubule-dependent quality control compartment in the ER. *Am J Physiol-Cell Physiol* 2011; **301**: C75-C85.

Supplementary Information accompanies the paper on the Oncogene website (http://www.nature.com/onc)